

This is a digital document from the collections of the *Wyoming Water Resources Data System (WRDS) Library*.

For additional information about this document and the document conversion process, please contact WRDS at wrd@uwyo.edu and include the phrase “**Digital Documents**” in your subject heading.

To view other documents please visit the WRDS Library online at:
<http://library.wrd.uwyo.edu>

Mailing Address:

Water Resources Data System
University of Wyoming, Dept 3943
1000 E University Avenue
Laramie, WY 82071

Physical Address:

Wyoming Hall, Room 249
University of Wyoming
Laramie, WY 82071

Phone: (307) 766-6651

Fax: (307) 766-3785

Funding for WRDS and the creation of this electronic document was provided by the Wyoming Water Development Commission
(<http://wwdc.state.wy.us>)

Water Resources Series No. 70

SOIL HYDRAULIC PROPERTIES
DETERMINED BY INFILTRATION
EXPERIMENTS AND SIMULATION

Wayland J. Anderson
Warren G. Hedstrom

November 1977

Completion Report
to
Office of Water Research and Technology
U.S. Department of the Interior

Project A-007-WYO
Agreement 14-31-0001-3551, 3851

Research on which this paper is based was funded in part by a grant from the Office of Water Research and Technology, U.S. Department of the Interior, under Public Law 88-379, the Water Resources Research Act of 1964, acting through the Wyoming Water Resources Research Institute.

ABSTRACT

The objective of this study was to develop and test a method for determining the water content - matric potential relationship and the hydraulic conductivity - matric potential relationship for infiltration into soil. A computer program developed to solve the Richards equation used these relationships to simulate infiltration into soil under various conditions.

Evaluation of the proposed method consisted of conducting several infiltration experiments using soil columns from which infiltration rate-time data, the initial and final water contents, and an estimate of the hydraulic conductivity at the final water content were obtained. Simulation of the infiltration tests was performed by the computer using various parameters including the bubbling matric potential, pore size distribution index, transition values on the $\theta(h)$ curve, and the hydraulic conductivity at the final water content in the previously mentioned relationship. The parameters were varied until the simulated and observed infiltration rate-time relationships agreed closely. Experimental tests were also run to determine the agreement of these parameters to those resulting from the simulation.

Results showed that the proposed method can be used to determine the above relationships by numerical simulation of infiltration.

ACKNOWLEDGMENT

The Wyoming Water Resources Research Institute supported this study through OWRR Project Number A-007-WYO and this financial support is gratefully acknowledged.

CONTENTS

	<u>Page</u>
I. INTRODUCTION	1
Present Level of Research	2
Objectives.	3
II. BACKGROUND	4
Soil Water Potential.	4
Equations for Soil Water Movement	6
Infiltration Equations.	8
Determination of $K(\theta)$ and $D(\theta)$ Relationships. . .	13
III. NUMERICAL SOLUTIONS OF THE RICHARDS EQUATION	16
IV. EXPERIMENTAL PROCEDURE	24
Determination of the Infiltration Rate-Time Relationship.	24
Determination of $S(h)$	26
Determination of $K(h)$	29
V. RESULTS AND DISCUSSION	31
Agreement of Observed and Calculated Infiltration Relationships	31
Movement of Wetting Front	32
Effects of Parameters on Curve Variation.	32
Observed $\theta(h)$ Relationships	39
Reason for Discrepancies between Observed and Calculated Curves	39

	<u>Page</u>
VI. SUMMARY AND CONCLUSIONS.	43
Summary	43
Conclusions	44
Recommendations for Future Study.	45
SELECTED REFERENCES.	47
APPENDIX A: Derivation of Diffusivity Equation Used in INFIL Computer Program	50
APPENDIX B: Computer Program INFIL.	54
APPENDIX C: Test Data	72

LIST OF FIGURES

<u>Figure</u>	<u>Page</u>
1. The infiltration moisture profile	10
2. Graph showing laboratory infiltration curve and computer calculated infiltration curve.	18
3. Graph showing effective saturation versus matric potential	20
4. Graph showing relative hydraulic conductivity versus matric potential	22
5. Apparatus for determining the infiltration rate- time relationship	25
6. Apparatus for determining the saturated hydraulic conductivity.	26
7. Apparatus for saturating sample for K(h) test	26
8. Method to determine saturation and water content.	27
9. Constant head reservoir and device for deter- mining K(h)	28
10. Apparatus for determining hydraulic conductivity.	29
11. Apparatus for determining K(h) function	30
12. Observed and calculated infiltration curves for medium sandy loam	33
13. Observed and calculated infiltration curves for medium sandy soil	34
14. Observed and calculated infiltration curves for medium sandy soil	34
15. Observed and calculated infiltration curves for medium sandy soil	35
16. Observed and calculated infiltration curves for fine sandy soil	35
17. Wetting front movement for medium sandy soil.	36

<u>Figure</u>	<u>Page</u>
18. Wetting front movement for fine sandy soil.	36
19. Effects of Brooks-Corey and King intercept on the infiltration curve.	37
20. Effects of matric bubbling potential on the infil- tration curve	38
21. Effects of λ variation on the infiltration curve. . .	38
22. Effective saturation curve for tests 2-4.	40
23. Effective saturation curve for test 5	40
24. Variation of bulk density within the test column. . .	42

I. INTRODUCTION

Man's dependence upon soil and water resources for food production has been evident throughout history. As population increases, the demand for food and fiber becomes greater. To meet this demand, more attention is being directed to agricultural production in arid and semi-arid areas of the world. Here, the problem of maximizing the efficiency of water use, either under dryland farming methods or irrigation, is of increasing concern.

Agriculture uses 94 percent of the total annual quantity of water consumed by the United States (Chow, 1964). As municipal and industrial demands increase, competition for the water presently used by agriculture will become keener. Agriculture's increasing need for water must be met primarily by more efficient use, which will enable agriculture to be more competitive with municipal and industrial demands for the water resource.

In their efforts to improve water-use efficiency, agricultural and water resource engineers seek to understand, regulate, and modify the hydrologic cycle. One of the primary methods man uses to modify the cycle is irrigation. Of particular interest is the process of infiltration, the movement of water through the soil surface and vertically downward into the soil matrix. This process is of considerable practical importance, as the rate of infiltration determines the amount of water available for crops, as well as the water remaining for surface runoff. A better understanding of the infiltration process, therefore, should lead to development of farming practices which lower surface

runoff and deep percolation losses and thereby increase irrigation efficiency. This would result in an improvement in the quality of irrigation return flows, as well as a possible reduction in the water required for irrigation.

Present Level of Research

The phenomenon of water infiltration is a complex process. Both theoretical and empirical equations have been developed to express the infiltration rate as a function of various parameters and to provide a method for predicting infiltration rates. However, the parameters in any particular equation vary considerably due to differences in soils and initial moisture contents, and crusting and sealing effects at the surface. Also, these parameters are usually not related to the soil hydraulic properties. Thus, application of these equations involves determination of the parameters for each new set of conditions encountered.

A more theoretical approach is to apply the equation presented by Richards (1931), who combined the equation of continuity and Darcy's Law. This second-order nonlinear differential equation describes steady and unsteady flow in both saturated and partially saturated soils. However, the mathematical difficulty of solving the Richards equation, except for very simple applications, has prevented its use for more complex problems. With the aid of modern computer technology, numerical procedures have been applied to approximate the solution of Richards' equation. This has made solution of infiltration problems possible.

Solution of the partial differential equations requires the interrelationship among hydraulic conductivity k , matric potential h , and water content θ . Past methods of determining the relationships have involved considerable time and use of laboratory equipment. Skaggs et al. (1970) utilized an empirical relationship developed by Gardner (1958) to relate conductivity and head. This procedure requires that head and water content relationship be determined in the laboratory.

The method developed herein applies Skaggs' approach and relationships developed by Brooks-Corey (1964) and King (1965) to relate head and moisture content, resulting in a computer program which generates the relationships of head, water content, and hydraulic conductivity and eliminates the need for laboratory determination of these relationships.

Objectives

The study had the following objectives:

1. To develop an approximate method for determining the head versus moisture content function of soils.
2. To apply the Brooks-Corey and King methods of relating head to moisture content in the Skaggs program.
3. To acquire infiltration-time data from experimental tests run in the laboratory on soil columns.
4. To compare the soil infiltration curve generated by the numerical solution with the experimentally acquired curve and thus test the validity of the program.
5. To evaluate the effects of the various soil hydraulic parameters on the infiltration rate.

II. BACKGROUND

The infiltration process has been analyzed from a variety of viewpoints, ranging from the strictly empirical to those involving rigorous application of theory. Although much of the early, more empirically oriented work produced solutions to various infiltration problems, the trend in recent years has been to apply the physical principles of soil water movement and to solve the differential equations of soil moisture flow. This discussion will briefly review the more significant aspects of both the empirical and theoretical approaches to the infiltration problem, including soil water potentials, equations for soil water movement, and infiltration equations. For a more complete review of the background material the reader is referred to Swartzendruber (1966), Childs (1969), and Hagan et al. (1967).

Soil Water Potential

The term "potential" as applied to soil water is a measure of the amount of work that must be done to transport water from a pool of pure water to the point under consideration. In other words, it represents the soil water's energy level which may have been produced by one or more of the forces that can act on soil water.

The types of soil water potentials are (1) matric potential, resulting from the presence of the solid phase; (2) osmotic potential, resulting from the effect of dissolved solutes; and (3) gravitational potential, resulting from gravitational forces.

Matric potential. Soil water at a pressure greater than atmospheric is considered to have a positive pressure potential. Similarly,

soil water at a pressure lower than atmospheric has a negative pressure potential. Thus, water at a horizontal free-water surface is at zero pressure potential, and water that has risen in a capillary tube is at a negative pressure potential.

Capillary pressure results from capillary forces developed by surface tension of water and is given by the capillary equation:

$$P_c = P_o - P_s = \sigma \left(\frac{1}{R_1} + \frac{1}{R_2} \right) , \quad (1)$$

where:

P_o = atmospheric pressure = 0,

P_s = soil water pressures, usually less than atmospheric in unsaturated soils,

P_c = pressure deficit of soil water or capillary pressure,

σ = surface tension of the water,

R_1, R_2 = principal radii of curvature of a point on the meniscus.

Not only capillary but also absorptive forces act upon soil water due to the soil matrix. Absorptive forces result from the attraction of water to soil particles. The effects of both forces result in the development of the matric potential, h .

Osmotic potential. Osmotic potential results from solutes in the soil solution and their movement across a semipermeable membrane such as root cell walls. This potential will be neglected in this study because it does not apply to water flowing from point to point within the soil matrix.

Gravitational potential. The gravitational potential, z , of soil water results from the force of gravity acting upon soil water. It is

determined by the soil water elevation at a particular point with respect to an arbitrary reference level, generally selected below the soil column to maintain a positive or zero potential.

Total potential. Total potential h in this study is considered to consist of the matric potential and gravitational potential and is constant in a static system. In a dynamic system a total potential gradient is present, causing water movement in the direction of lower total potential.

Equations for Soil Water Movement

The equations that have been developed to evaluate soil water movement are (1) those for flow through saturated soil, (2) those for flow through unsaturated soil, (3) the Richards equation, and (4) the diffusivity equation.

Flow through saturated soil. The flow of soil water in saturated soil is proportional to the potential gradient. The flow direction is opposite to the direction of total potential gradient. Darcy (1856) developed an equation for saturated conditions which is written here in a more generalized form:

$$q = -K \nabla H \quad , \quad (2)$$

where:

q = flux density or total flow/area,

K = saturated hydraulic conductivity,

∇H = gradient of total potential.

Flow through unsaturated soil. The flow through unsaturated soil differs from saturated flow because some pores are air-filled, reducing

the flow area, and the hydraulic conductivity becomes dependent upon water content. Buckingham (1907) expressed hydraulic conductivity as a function of volumetric water content for unsaturated flow on the basis of arguments developed for heat and electrical flow.

Richards' equation for soil water flow. Richards (1931) combined the continuity equation,

$$\frac{\partial \theta}{\partial t} = -\nabla \cdot \vec{q} \quad , \quad (3)$$

and Darcy's law, altered for unsaturated flow,

$$\vec{q} = -K(\theta) \nabla H \quad , \quad (4)$$

to obtain his equation

$$\frac{\partial \theta}{\partial t} = \nabla \cdot (K(\theta) \nabla H) \quad (5)$$

for flow in unsaturated soil.

Diffusivity equation for soil water flow. To assist in solving the flow equation developed by Richards, a function was introduced by Childs and Collis-George (1950) termed diffusivity $D(\theta)$ and defined as

$$D(\theta) = K(\theta) \frac{dh}{d\theta} = K(\theta) / (d\theta/dh) \quad , \quad (6)$$

where $d\theta/dh$ is the soil water capacity. Incorporating diffusivity into the Darcy equation (equation 4) results in

$$\vec{q} = D(\theta) \nabla \theta \quad . \quad (7)$$

Introducing the diffusivity term into the Richards equation (equation 5) gives

$$\frac{\partial \theta}{\partial t} = \frac{\partial}{\partial x} \left(D(\theta) \frac{\partial \theta}{\partial x} \right) , \quad (8)$$

resulting in

$$\frac{\partial \theta}{\partial t} = D(\theta) \frac{\partial^2 \theta}{\partial x^2} \quad (9)$$

for horizontal flow.

Infiltration Equations

The equations developed to describe infiltration dependence upon time and cumulative infiltration have been empirical and numerical in nature.

Empirically based infiltration equations. An early study of infiltration rates and volumes was made by Green and Ampt (1911). They assumed that a distinct and precisely definable wetting front could be observed and the matric potential at the wetting front remained nearly constant. Their equation is

$$f = A \left(1 + \frac{B' (P + H)}{F} \right) , \quad (10)$$

where:

f = infiltration rate,

F = accumulative infiltration,

H - depth of ponding at surface,

P = matric potential at the wetting front,

A, B' = constants dependent on soil type and conditions.

The first investigator to successfully fit an empirically developed curve to actual field infiltration data was Kostikov (1932). His equation is

$$f = K t^a , \quad (11)$$

where:

f = as previously defined,

t = time,

K, a = empirical constants.

An equation that has been widely used in hydrology was developed by Horton (1940). His equation is

$$f = F_c + (F_o - F_c) e^{-K_f t} , \quad (12)$$

where:

f = as previously defined,

t = time,

F_c = steady state infiltration rate over long periods,

F_o = initial infiltration rate at $T = 0$,

K_f = a constant depending on soil and surface conditions.

This equation requires that the relationships between F_c and rainfall intensity and between K_f and rainfall intensity be known.

The soil moisture profile during vertical infiltration was studied by Bodman and Coleman (1944), whose results are shown in Figure 1.

The saturation zone is adjacent to the soil surface. The transition zone, a region which decreases in soil water content, extends from the saturation zone to the transmission zone, a region of nearly constant water content which lengthens as infiltration continues. The wetting zone is a region of rapid soil water content change ending at the wetting front, which is the visible limit of water penetration into the

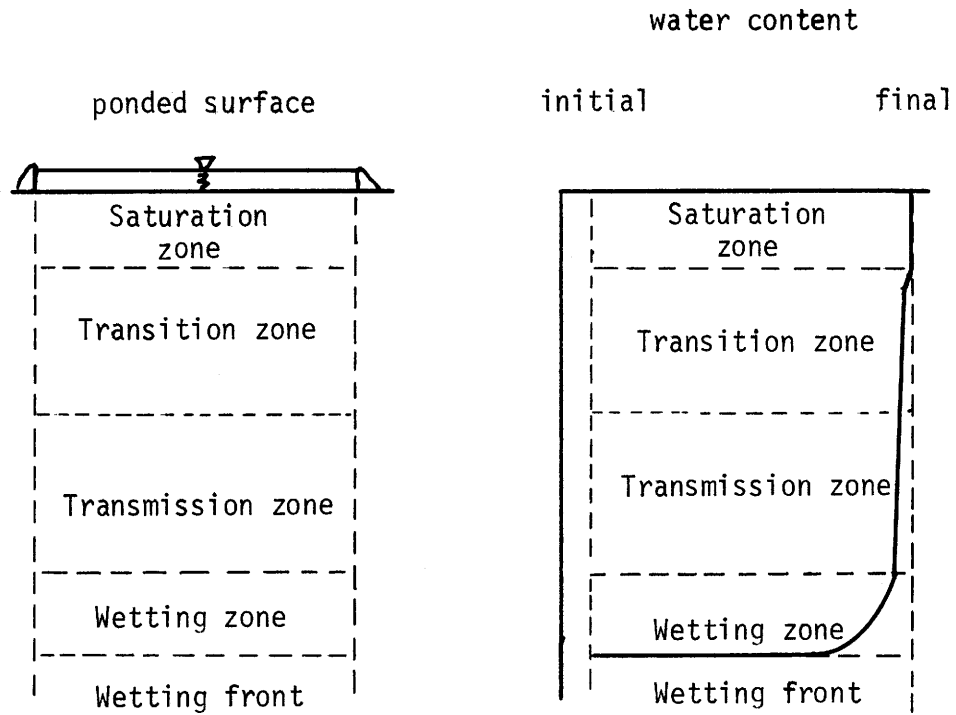


Figure 1. The infiltration moisture profile. Left shows section of profile; right, the water content versus depth curve.

soil. They explained the decrease in infiltration rate with time as a result of the decrease in the total potential gradient.

Kirkham and Feng (1949) studied the wetting front advance for horizontal infiltration and noted that the distance to the wetting front is proportional to the square root of time required to reach that distance.

Holtan (1961) used the concept of storage potential, or the maximum amount of water between saturation and the wilting point moisture content. His equation is

$$f = a(S_t - F) n + F_c \quad , \quad (13)$$

where:

f and F_c = as previously defined,

S_t = storage potential of the soil (saturated minus initial moisture content),

a, n = constants dependent on soil type and surface conditions.

As infiltration occurs, the storage capacity of the soil is decreased, reducing the pore volume available for storage of water.

Empirically based infiltration equations have utilized parameters that were not based on physical properties, making them difficult to apply universally. A more theoretical approach is to apply Richards' equation and relationships involving soil hydraulic properties in solving infiltration problems.

Analytical and numerical solutions to the Richards equation.

Numerical solutions to the infiltration process have involved solving the Richards equation for flow. The relationship between permeability, or preferably hydraulic conductivity, and the moisture content of the soil must be known.

Klute (1952) applied the Boltzman transformation

$$\phi = Xt^{-1/2}, \quad (14)$$

where:

X = horizontal distance,

t = time,

to the Richards equation for horizontal infiltration, which is

$$\frac{\partial \theta}{\partial x} = \frac{\partial}{\partial x} \left(D(\theta) \frac{\partial \theta}{\partial x} \right) . \quad (15)$$

The application of this transformation yielded the following ordinary differential equation:

$$-\frac{\phi}{2} \frac{d\theta}{d\phi} = \frac{d}{d\phi} \left(D(\theta) \frac{d\theta}{d\phi} \right) \quad (16)$$

Klute (1952) used a numerical solution developed by Crank and Henry (1949) to solve equation 16.

Philip (1957) also applied this Boltzman transformation to solve the Richards equation for vertical infiltration by an iterative procedure and obtained a solution in the form of a power series in $t^{1/2}$:

$$X = t^{-1/2} + \chi t + \psi t^{3/2} + \omega t^2 + \dots + f_m(\theta) t^{m/2} + \dots \quad (17)$$

Diffusivity is represented by a polynomial function of θ , because matric potential and hydraulic conductivity are both assumed to be single-valued functions of water content. Philip's equation produced good results for distribution of water content. Verification of the Klute and Phillip approach was made by Young (1957) and Peck (1964), who both used glass beads and slate dust.

Numerical solution of Richards' equation in finite-difference form.

Hanks and Bowers (1962) were the first investigators to develop a finite-difference solution of Richards' equation. This application was made for ponded vertical infiltration of water into soil having non-uniform initial moisture content. They used actual field soil water content values along with the $D(\theta)$ and $h(\theta)$ relationships determined in the laboratory from core samples.

Rubin and Steinhardt (1963) applied Richards' equation for constant rainfall rate using the finite-difference approach in their

computer solution. They utilized fitted empirical equations for $h(\theta)$ and $K(\theta)$ relationships developed by Gardner (1958).

Richards' equation was applied for vertical infiltration into nonhomogeneous soils having nonuniform initial moisture content and hysteresis by Whistler and Klute (1966). They used theories and resultant equations developed by Childs and Collis-George (1950) and Millington and Quirk (1959) for the $h(\theta)$ and $K(\theta)$ relationships.

Determination of $K(\theta)$ and $D(\theta)$ Relationships

The first measurement of hydraulic conductivity as a function of matric potential was made by Richards (1931). He used a tensiometer to supply water at a negative pressure to a soil sample and then extracted it by another tensiometer at negative pressure. Additional tensiometers were used to measure the matric potential within the horizontal column.

Moore (1939) measured the matric potential along the column and then measured the moisture content at the end of the experiment. He succeeded in determining the moisture content and potential gradient at a point.

Childs and Collis-George (1950) were the first investigators to show that unsaturated hydraulic conductivity was related to pore size distribution.

Millington and Quirk (1959) developed an approach dividing the moisture characteristic curve into equal segments, then averaged the pressure within the segment. As the soil drained, moisture content decreased, removing certain pore classes and the accompanying pressure classes from their equation.

Gardner (1958) developed an empirical equation relating diffusivity to water content. His equation is

$$D(\theta) = a e^{B \theta} , \quad (18)$$

where:

$$\begin{aligned} D(\theta) &= \text{diffusivity,} \\ \theta &= \text{water content,} \\ a &= \text{diffusivity at } \theta = 0. \end{aligned}$$

Gardner (1958) also developed an equation relating matric potential and hydraulic conductivity:

$$K(h) = ((h/h_1)^a + b)^{-1} , \quad (19)$$

where:

$$\begin{aligned} K(h) &= \text{as previously defined,} \\ a, b &= \text{constants in equation,} \\ h &= \text{matric potential,} \\ h_1 &= \text{parameter related to mean pore size.} \end{aligned}$$

Brooks and Corey (1964) developed an equation relating matric potential and hydraulic conductivity. Their equation is

$$K_r = K_s (P_b/P_c)^\eta , \quad (20)$$

where:

$$\begin{aligned} K_r &= \text{relative hydraulic conductivity, ratio of hydraulic} \\ &\quad \text{conductivity to that of saturated hydraulic conduc-} \\ &\quad \text{tivity,} \\ K_s &= \text{saturated hydraulic conductivity,} \\ P_b &= \text{bubbling matric potential,} \end{aligned}$$

P_c = matric potential,

η = soil parameter related to pore size distribution.

King (1965) proposed an equation relating matric potential and hydraulic conductivity for imbibition. His equation is

$$K_r = \frac{\sigma(\cosh((P_c/P_2)^{\eta/2}) - 1)}{(\cosh((P_c/P_2)^{\eta/2}) + 1)}, \quad (21)$$

where:

K_r = as previously defined,

σ = constant ≈ 1 ,

P_c = matric potential,

P_2 = bubbling matric potential,

η = as previously defined.

As discussed above, methods have been developed for determining the relationships between hydraulic conductivity and water content and between diffusivity and water content. Empirical equations have been presented which provide a representation of these relationships. Laboratory techniques for obtaining data for the above relationships are generally time-consuming and expensive. Also, the determination of various parameters in the equations reviewed involves plotting data and the use of judgment. Therefore, the development of a more direct approach in determining the relationships among the hydraulic properties of a soil appears to be a worthwhile step.

III. NUMERICAL SOLUTIONS OF THE RICHARDS EQUATION

As presented above, the Richards equation for vertical infiltration is

$$\frac{\partial \theta}{\partial t} = \frac{\partial}{\partial x} \left(D(\theta) \frac{\partial K}{\partial x} \right), \quad (8)$$

x being directed vertically downward. The solution to this equation is achieved by using the finite-difference approach. The left side of equation 8 may be written in finite-difference form as

$$\frac{\partial \theta}{\partial t} \approx (\theta_i^j - \theta_i^{j-1}) \frac{1}{\Delta t}, \quad (22)$$

where:

θ = as previously defined,

i = subscript denoting sequence number of depth increment,

j = superscript denoting sequence number of time,

Δt = time increment.

The right side of equation 8 can be written in a three-point central difference approximation of the derivatives with respect to x as

$$\begin{aligned} \frac{\partial}{\partial x} \left(D(\theta) \frac{\partial \theta}{\partial x} \right) - \frac{\partial K}{\partial x} \approx D_i^j (\theta_{i-1}^j - 2\theta_i^j + \theta_{i+1}^j) \frac{1}{\Delta x^2} \\ + (\theta_{i+1}^j - \theta_{i-1}^j) (D_{i+1}^j - D_{i-1}^j) \frac{1}{4\Delta x^2} - (K_{i+1}^j - K_{i-1}^j) \frac{1}{2\Delta x} \end{aligned} \quad (23)$$

Combining equations 22 and 23, equation 10 can be written in finite-difference form as

$$\begin{aligned}
(\theta_i^j - \theta_i^{j-1}) \frac{1}{\Delta t} &= D_i^j (\theta_i^j - 2\theta_{i-1}^j + \theta_{i+1}^j) \frac{1}{x^2} + (\theta_{i+1}^j - \theta_{i-1}^j) \\
(D_{i+1}^j - D_{i-1}^j) \frac{1}{4x^2} - (K_{i+1}^j - K_{i-1}^j) \frac{1}{2\Delta x} &. \tag{24}
\end{aligned}$$

By combining terms, equation 24 can be written as

$$A_i^j \theta_{i-1}^j + B_i^j \theta_i^j + C_i^j \theta_{i+1}^j = d_i^j ,$$

where:

$$A_i^j = (4D_i^j + D_{i+1}^j - D_{i-1}^j) \frac{1}{4\Delta x^2} , \tag{25}$$

$$B_i^j = -2 D_i^j \frac{1}{\Delta x^2} - \frac{1}{\Delta t} , \tag{26}$$

$$C_i^j = (4D_i^j - D_{i+1}^j + D_{i-1}^j) \frac{1}{4\Delta x^2} , \tag{27}$$

$$d_i^j = (K_{i+1}^j - K_{i-1}^j) \frac{1}{2\Delta x} \theta_i^{j-1} \frac{1}{\Delta t} . \tag{28}$$

Solving the finite-difference equation involves expressing coefficients A, B, C, and d for the time step j in terms of the soil properties for that time step and the θ values for the previous, j-1, time step. Equation 24 can be written for each interior node at time j, producing m-2 equations in m unknowns. Two additional equations utilizing the boundary conditions at x=0 and x=L may be used. The resultant tridiagonal matrix can be solved by using a technique developed by Richtmyer (1957). A solution for the finite j=2 and the next time step is considered next.

The terms D_i^j and K_i^j are dependent upon θ_i^j . However, in the solution, the θ_i^{j-1} is used to determine the soil properties D_i^{j-1} and K_i^{j-1} , which are in turn used to determine the θ_i^j values. An iteration process

is continued until the moisture contents used are functionally consistent with the values of the θ_i^j 's obtained.

The soil properties used in this study were interrelated by empirical equations developed by Brooks-Corey (equation 20) and King (equation 21). These were combined because of the poor fit of experimental data below the bubbling pressure produced by the Brooks-Corey equation 20. The King equation 21 was used to fit this portion of the data.

This study found that the $K(h)$ and $h(\theta)$ relationships can be best represented by a combination of the Brooks-Corey 20 and King 21 equations. The procedure consists of obtaining the parameters in the Brooks-Corey and King equations which produce the minimum area between the laboratory infiltration curve and the computer calculated infiltration curve as shown in Figure 2.

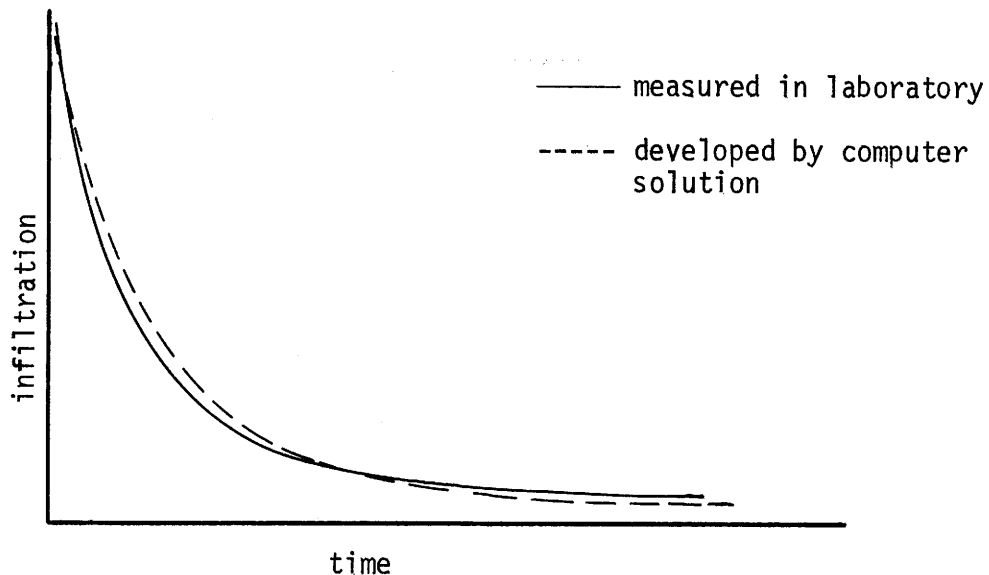


Figure 2. Graph showing laboratory infiltration curve and computer calculated infiltration curve.

The Brooks-Corey (1964) equation relating effective saturation and matric potential is

$$\begin{aligned}
 S_e &= 1.0 && \text{for } P_c \leq P_b \text{ ,} \\
 S_e &= (P_b/P_c P)^{\lambda_1} && \text{for } P_c \geq P_b \text{ ,}
 \end{aligned}
 \tag{29}$$

where:

$$\begin{aligned}
 S_e &= \text{effective saturation or} \\
 S_e &= (S - S_r) / (1.0 - S_r) \text{ ,}
 \end{aligned}
 \tag{30}$$

S = saturation,

S_r = residual saturation, saturation for very large matric potential values,

P_b = bubbling matric potential,

P_c = matric potential,

λ_1 = pore size distribution index.

The Brooks-Corey relationship (equation 29) produces two straight lines on logarithmic graph paper having an intercept of $P_c = P_b$, at $S_e = 1.0$. This straight line does not account for the zone of relatively constant effective saturation observed from laboratory data below P_b as shown in Figure 3.

The King equation 31 is used to develop values for S_e greater than 0.5. This value was chosen because of the tendency of the laboratory data to diverge from the straight line relationship near this point. The matric potential for an S_e value of 0.5 in the Brooks-Corey equation is substituted into the King equation 30 and the new bubbling pressure is determined in the King equation to produce a continuous curve relating effective saturation and matric potential. The equation is

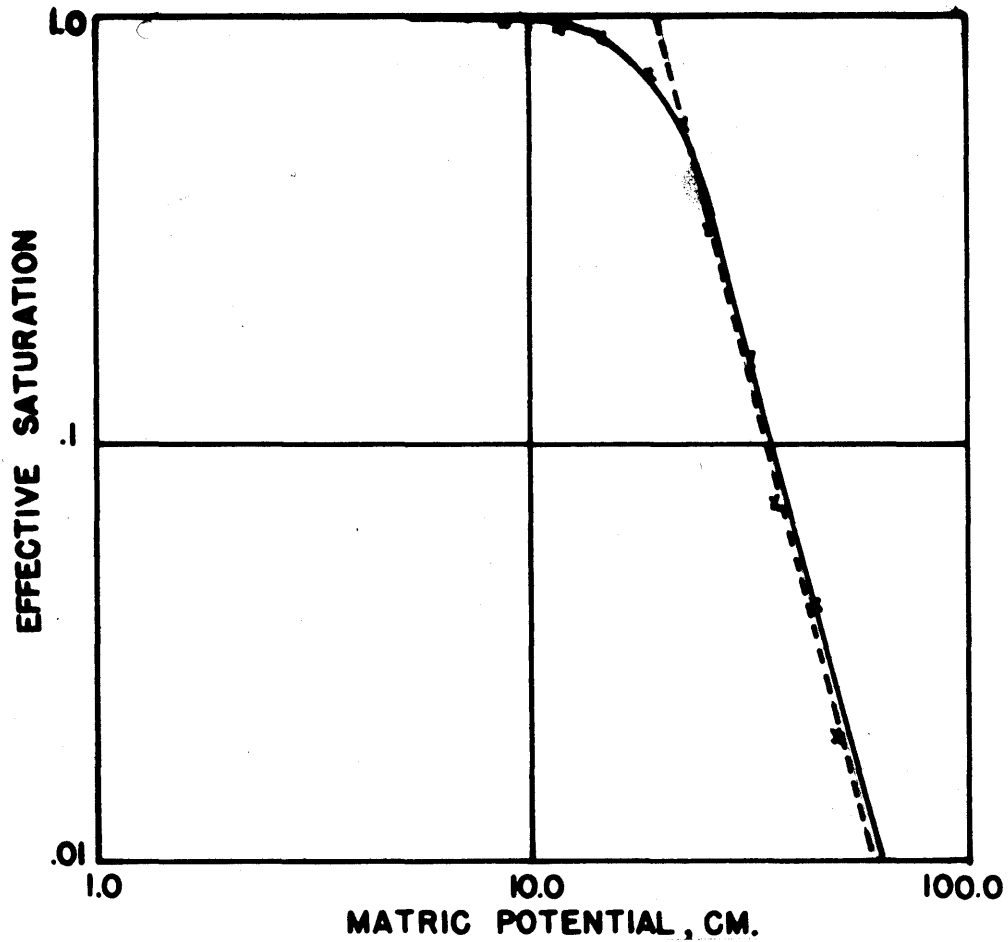


Figure 3. Graph showing Brooks-Corey (----), King (—), and laboratory data (xxx) for effective saturation versus matric potential.

$$S_e = (\cosh(P_c/P_2)^{\lambda_2} - 1.0) / (\cosh(P_c/P_2)^{\lambda_2} + 1.0) \quad (31)$$

where:

S_e = as previously defined,

P_c = matric potential,

P_2 = the parameter in the King equation,

$\lambda_2 = 1/2 \lambda_1$.

Equation 30 can be rearranged in the following form:

$$S = S_e(1.0 - S_r) + S_r \quad (32)$$

Water content is related by

$$\theta = P \times S \quad , \quad (33)$$

where:

θ, S = as previously defined,

P = porosity or maximum water content obtained immediately after infiltration.

Brooks-Corey (1964) also developed an empirical equation for relative hydraulic conductivity and matric potential. Their equation is

$$K_r = (P_b/P_c)^{\eta_1} \quad , \quad (34)$$

where:

K_r = as previously defined,

P_c, P_b = as previously stated,

η = slope of curve and related to λ , by $\eta_1 = 2 + 3\lambda_1$.

This relationship (equation 34) also produces a straight line on logarithmic graph paper which has an intercept of $P_c = P_b$ at $K_r = 1$. This straight line does not account for the zone of relatively constant relative hydraulic conductivity below P_b as shown in Figure 4. Results of Hanks and Bowers (1962) show that it is important to accurately describe this region for good prediction of partially saturated flow during imbibition.

To predict the relationship below the bubbling pressure in the region of relatively constant hydraulic conductivity, the King equation 35 is used to develop relative hydraulic conductivity values by utilizing the King bubbling pressure from equation 31. The equation is

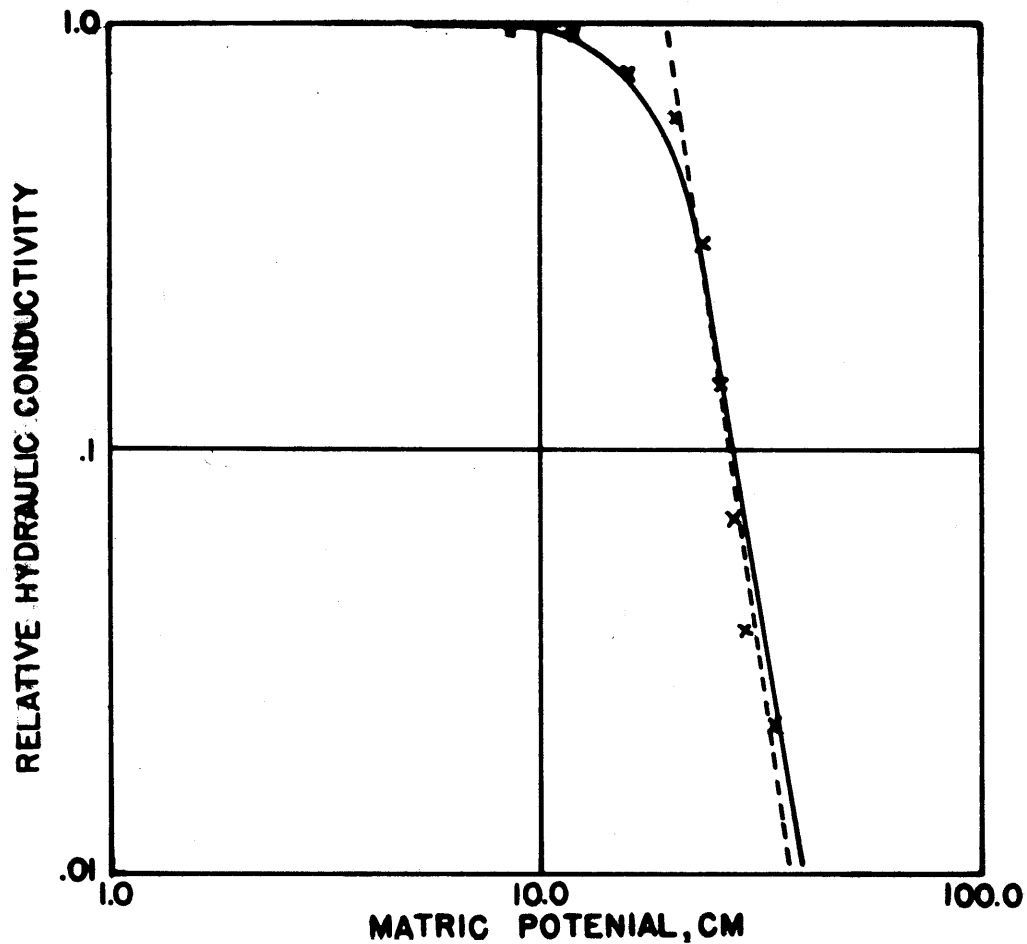


Figure 4. Graph showing Brooks-Corey (----), King (—), and laboratory data (xxx) for relative hydraulic conductivity versus matric potential.

$$K_r = [\cosh ((P_c/P_2)^{\eta_2}) - 1] / [\cosh ((P_c/P_2)^{\eta_2}) + 1] , \quad (35)$$

where:

K_r, P_c, P_2 = as previously defined,

$$\eta_2 = 1/2 \eta .$$

Hydraulic conductivity is determined by multiplying relative conductivity by saturated conductivity.

The parameters λ_1, λ_2 and η_1, η_2 for the equations for $S_e(P_c)$ 29 and 31 and the equations for $K_r(P_c)$ 34 and 35 can be related by a relationship developed by Brooks-Corey (1964). It is

$$\eta_1 = 2 + 3\lambda_1 \quad , \quad (36)$$

where:

η_1 and λ_1 = as previously defined.

For this study, λ_2 was assumed to be one-half the slope of the $K_r(P_c)$ curve, resulting in the following equation relating λ_2 and η_2 :

$$\eta_2 = 1 + 3\lambda_2 \quad . \quad (37)$$

To solve the Richards equation for flow, diffusivity values must also be available. Since diffusivity is defined by

$$D(\theta) = K(\theta) \, dh/d\theta \quad ,$$

the values of $dh/d\theta$ approach infinity as S_e approaches 1.0, making necessary an empirical equation for diffusivity. It is

$$D(\theta) = \frac{P_b K_{sat}}{2\lambda_2} (\theta - \theta_r) \frac{(1 + 4\lambda_2)}{\lambda_2} (\theta_s - \theta_r) \frac{(-1 - 6\lambda_2)}{2\lambda_2} \quad , \quad (38)$$

where:

$D(\theta)$ = diffusivity,

λ_2, θ, P_b = as previously defined,

θ_s = saturated moisture content, P,

θ_r = residual moisture content ($P \times S_r$).

The derivation for equation 36 is presented in Appendix A.

IV. EXPERIMENTAL PROCEDURE

The objectives of the laboratory experiments were (1) to determine how well the Brooks-Corey and King relationships represent the experimental data of saturation versus matric potential $S(h)$ and hydraulic conductivity versus matric potential $K(h)$; and (2) to determine the values of the parameters in the Brooks-Corey and King equations by varying these parameters in the computer program INFIL, by producing the minimum area between the calculated and experimental curves. The experimental facilities consisted of equipment to determine the $S(h)$ and $K(h)$ functions and equipment to study the infiltration rate-time relationship of a sandy soil.

Determination of the Infiltration Rate-Time Relationship

The infiltration rate-time relationship was determined from observation of infiltration into soil contained in a 4.5-inch (11.5 cm) O.D. plexiglass column shown in Figure 5. The soil was passed into the column through a tube initially extended to the bottom of the column and slowly raised and moved in a circular motion as the soil was deposited. The column was usually filled to a soil height of 40-50 cm. The column was then weighed and the bulk density was determined. A uniform initial moisture content within the column was obtained by adding distilled water to the soil and thoroughly mixing it.

A constant head reservoir was used to supply water to the surface of the soil sample. The water was maintained at a constant level above the soil surface. The elevation of the water within the reservoir was observed at specific time intervals on a scale attached to the reservoir column. In this manner, data for the column-time rela-

tionship were obtained. The wetting front location was also observed at the same time intervals.

The saturated hydraulic conductivity was determined by measuring the outflow rate immediately after water began to flow from the bottom of the column, as shown in Figure 6. The constant ponding depth was maintained during this determination.

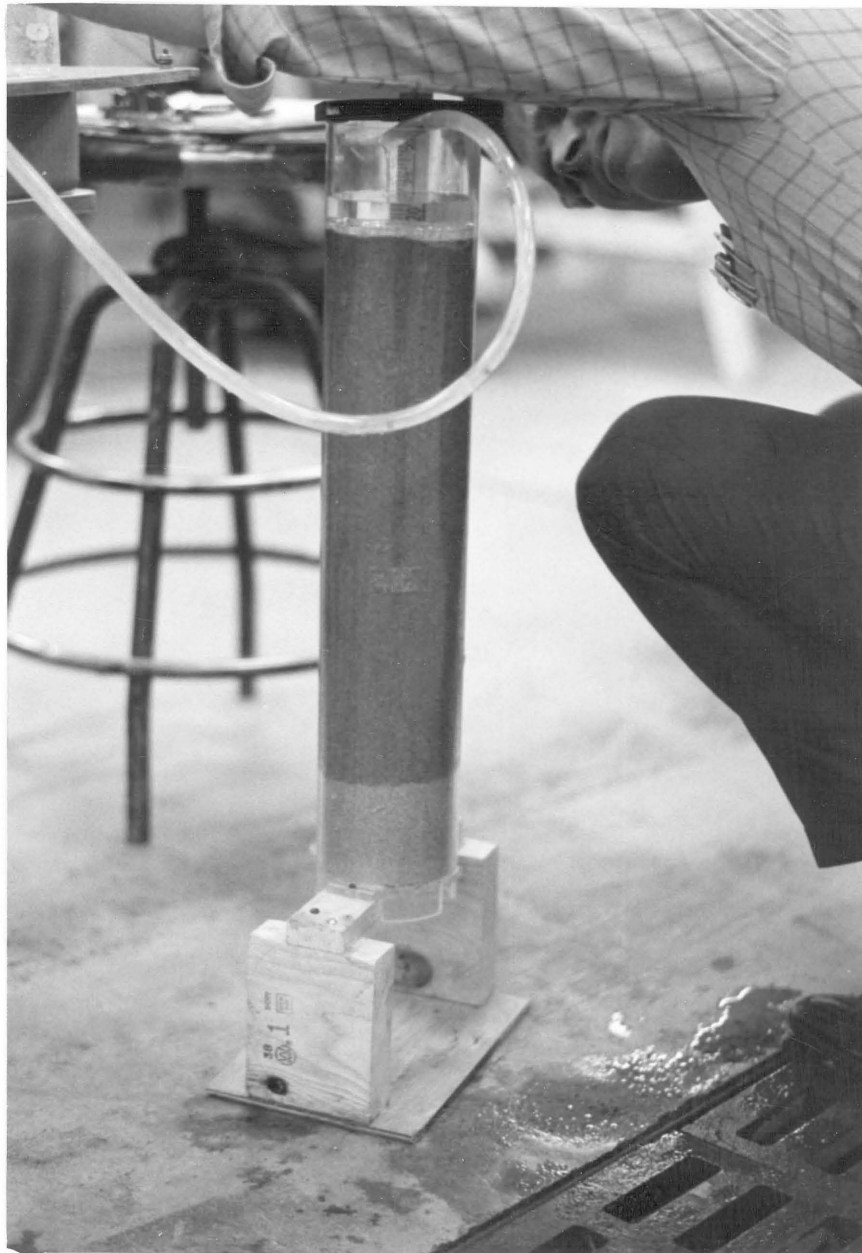


Figure 5. Apparatus for determining the infiltration rate-time relationship.

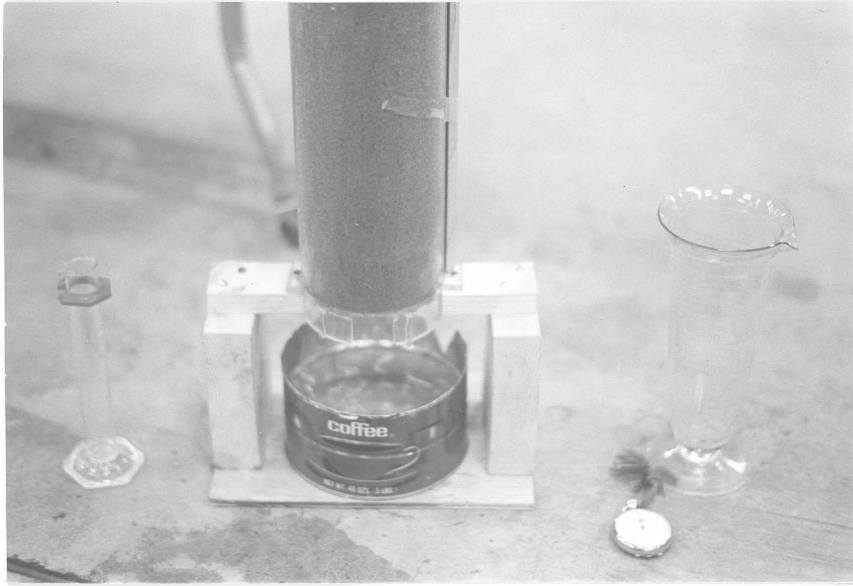


Figure 6.
Apparatus for
determining
the saturated
hydraulic
conductivity.

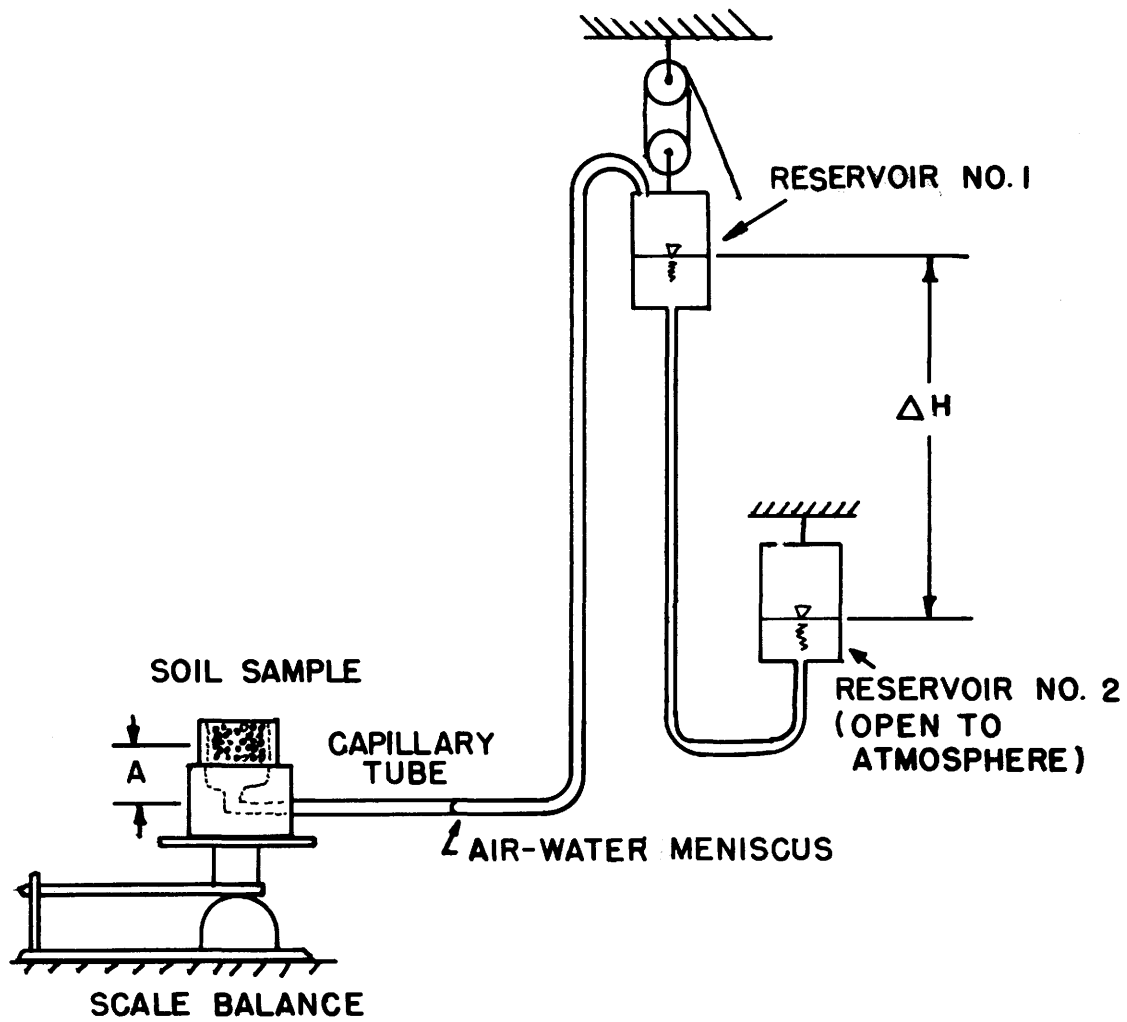
Determination of $S(h)$

A plexiglass column 1.65 cm in height and 10.87 cm I.D. was filled with the same soil used in the infiltration rate test. The soil was packed to the same density as the large column and saturated in the saturation chamber shown in Figure 7 to remove the entrapped air within the sample.



Figure 7.
Apparatus for
saturating
sample for
 $K(h)$ test.

Two reservoirs were mounted, with one on pulleys, as shown in Figure 8. Reservoir number one was elevated with respect to the other to increase the matric potential of the water in the soil sample. The sample was located on a scale balance to measure the accompanying change in water content determined by the change in weight.



$$\text{MATRIC POTENTIAL} = \Delta H + A + \text{CAPILLARY RISE}$$

Figure 8. Method to determine saturation and water content.

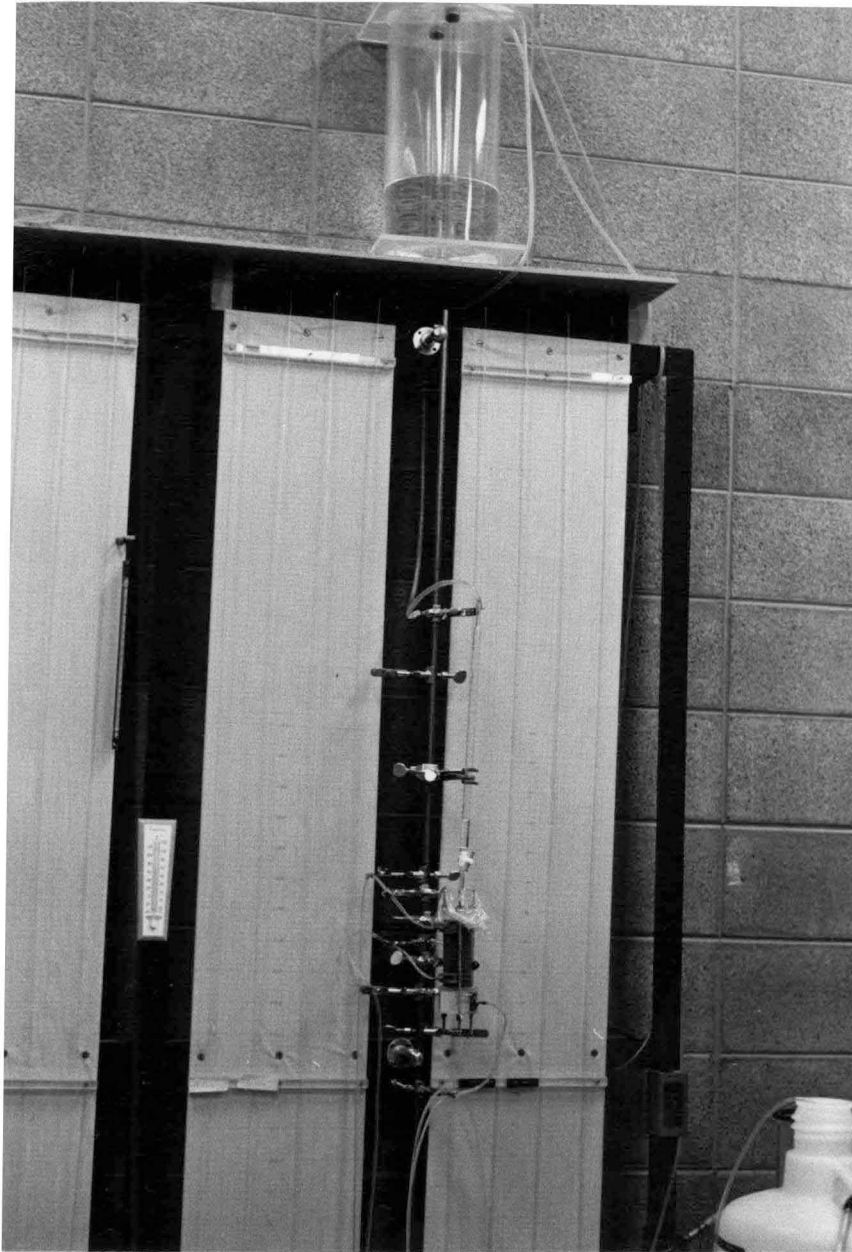


Figure 9. Constant head reservoir and device for determining $K(h)$.

Determination of $K(h)$

The method used to determine capillary pressure - hydraulic conductivity was developed by Anat et al. (1965). Figure 7 shows the plexiglass cylinder being saturated, and Figures 9 and 10 show the sample mounted and the constant head reservoir used to provide water to the sample. Figure 11 shows the tensiometers attached to the sample to provide data for determining the matric potential. The hydraulic gradient was determined by adding the matric potential for tensiometer one, H_1 , to the matric potential for tensiometer two, H_2 , and including the elevation difference for the tensiometers, L . The sum ($H_1 + H_2 + L$)

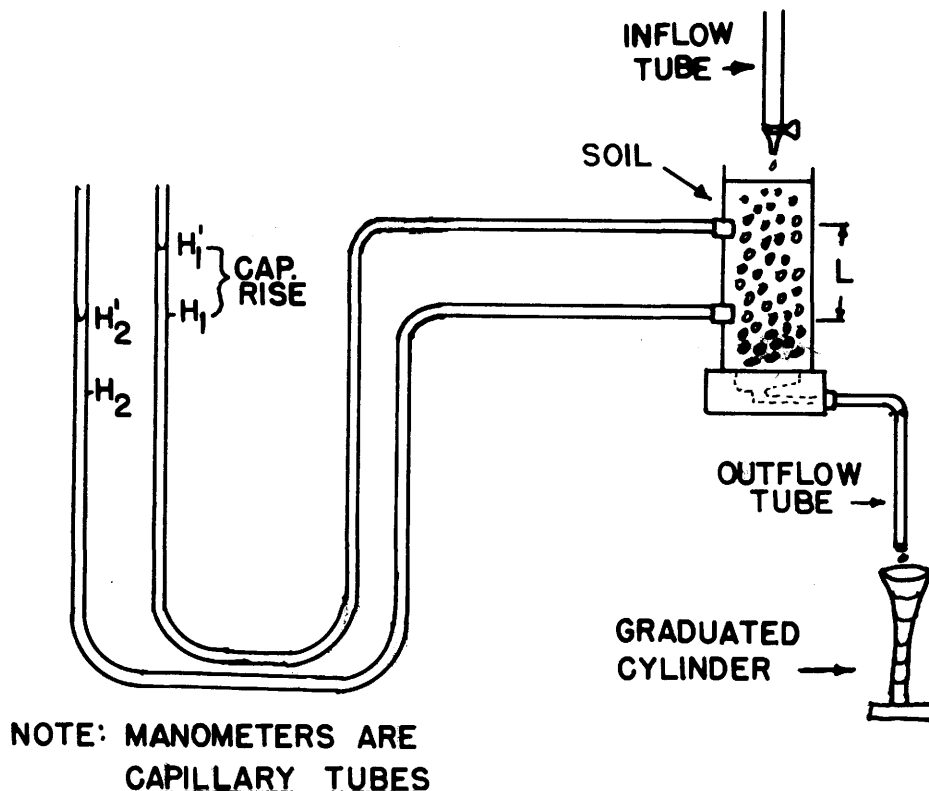


Figure 10. Apparatus for determining hydraulic conductivity as a function of matric potential.

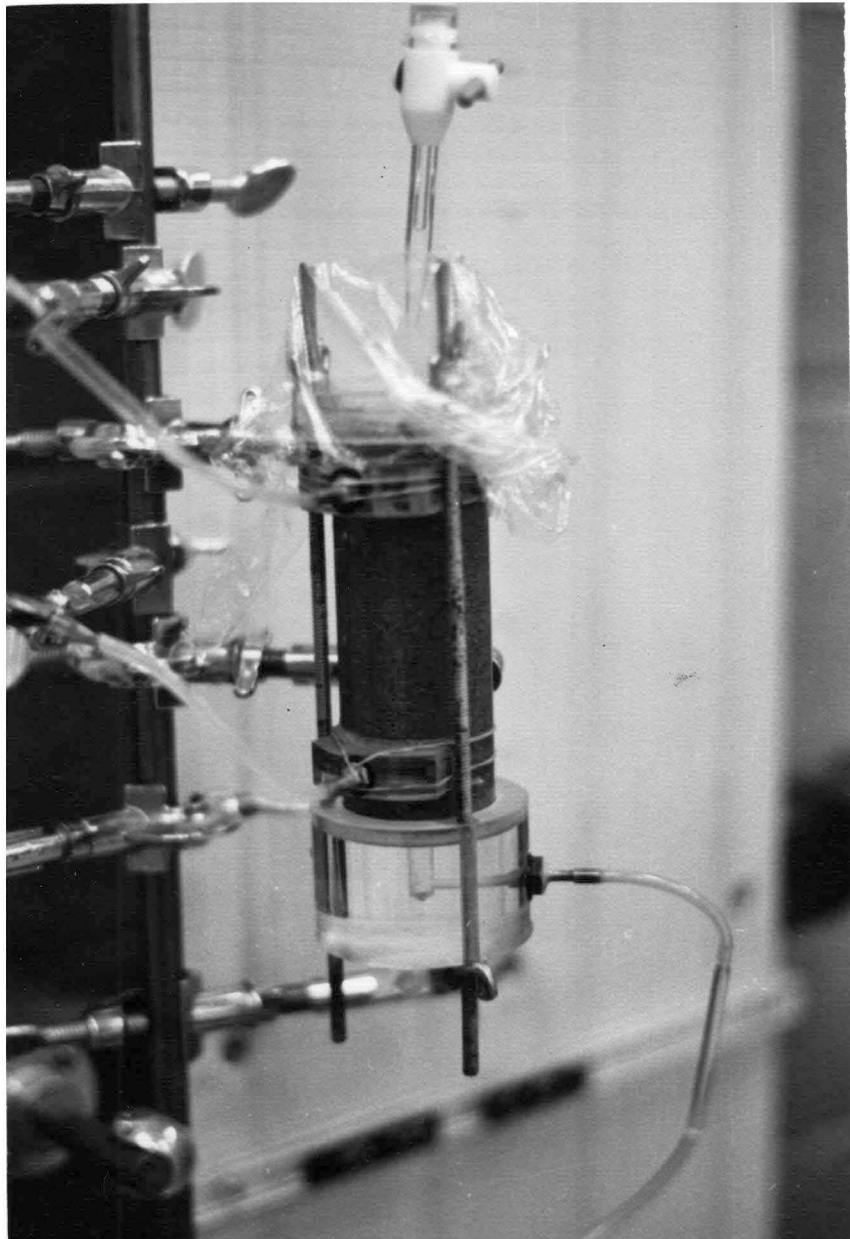


Figure 11. Apparatus for determining $K(h)$ function.

was then divided by the flow length, L , giving the hydraulic gradient. The flow rate was found by measuring the volume of water discharged from the outflow tube over a period of time. The resulting hydraulic conductivity was computed by dividing the flow rate by the hydraulic gradient.

After the data for $K(h)$ and $S(h)$ were acquired, the values were plotted to determine the bubbling matric potential as defined by Brooks-Corey (1964), the λ_1 and η_1 values from the slopes of the curves. The residual saturation, S_r , was determined by varying its value until the effective saturation versus matric potential function fell on a straight line.

V. RESULTS AND DISCUSSION

The objective of this study was to determine soil hydraulic properties by comparison of observed and calculated infiltration rate-time curves. Infiltration experiments were run on columns of medium sandy soil and fine sandy soil. These infiltration rate-time data were then simulated by the computer program INFIL using the $\theta(h)$ and $K(h)$ functions determined by the method given in Section III above. The computed and observed influx curves were compared to determine the reliability of the $\theta(h)$ and $K(h)$ functions to characterize the soil hydraulic properties for these two soils.

Agreement of Observed and Calculated Infiltration Relationships

Results of the observed and calculated infiltration rate-time and cumulative volume-time relationships into initially wet columns of

medium sandy soil and fine sandy soil are given in Table 1. Graphical results are given in Figures 12-16 (tests 1-5).

The calculated curves showed reasonable agreement for each of the tests run. Excellent agreement for all times was difficult to obtain owing to the difficulty in maintaining a homogeneous soil when loading the column used to observe infiltration rate-time values. Difficulty also was encountered in maintaining a uniform ponding depth on the surface of the soil column. It is possible that smaller particles may move from the upper area of the column down into the column, thus increasing the porosity in the upper column. This effect would tend to increase the variation in this calculated and observed infiltration rate-time curve for early times of infiltration.

Movement of Wetting Front

The movement of the wetting front was observed in all tests, with the results from test 4 and test 5 shown in Figures 17 and 18. Test 4 was chosen because it appeared to be the most representative test involving the medium-sand soil. Test 5 is for the fine-sand soil.

The agreement of the observed and calculated infiltration wetting front curves gave an indication of the validity of the $\theta(h)$ and $K(h)$ values determined by INFIL as shown by Figures 17 and 18. The agreement of the calculated and observed curves also indicated the accuracy of the initial and final moisture contents used as boundary conditions by INFIL.

Effects of Parameters on Curve Variation

The degree of coalescence of the calculated curves with the observed data was studied. It was determined that the parameters used in the

TABLE 1. Data and results for infiltration run

TEST NO.	SOIL*	INITIAL MOISTURE CONTENT	FINAL MOISTURE CONTENT	% WATER ADDED	BULK DENSITY (g/cc)	AGREEMENT OF CALCULATED AND OBSERVED INFILTRATION CURVES	DETERMINED SOIL HYDRAULIC PARAMETERS		
							λ	HTBB	EFVAL
1	Passing #30 Sieve	1%	46%	35%	1.46	92%	.50	81.2	.90
						88%	.50	20.9	.85
2	Passing #40 Sieve	3%	37%	34%	1.43	93%	.82	80.5	.93
						92%	.82	74.3	.93
3	Passing #40 Sieve	23%	39%	16%	1.46	59%	.80	84.7	.90
4	Passing #40 Sieve	2%	36%	34%	1.44	91%	.95	42.2	.80
						90%	.95	30.5	.80
5	Passing #60 Sieve	1%	25%	24%	1.43	92%	.95	31.1	.90
						60%	1.50	86.9	.90
						65%	1.25	86.9	.90

*Sieves are U.S. series. Sieve #30--.59 mm, #40--.42 mm, #60--.25 mm.

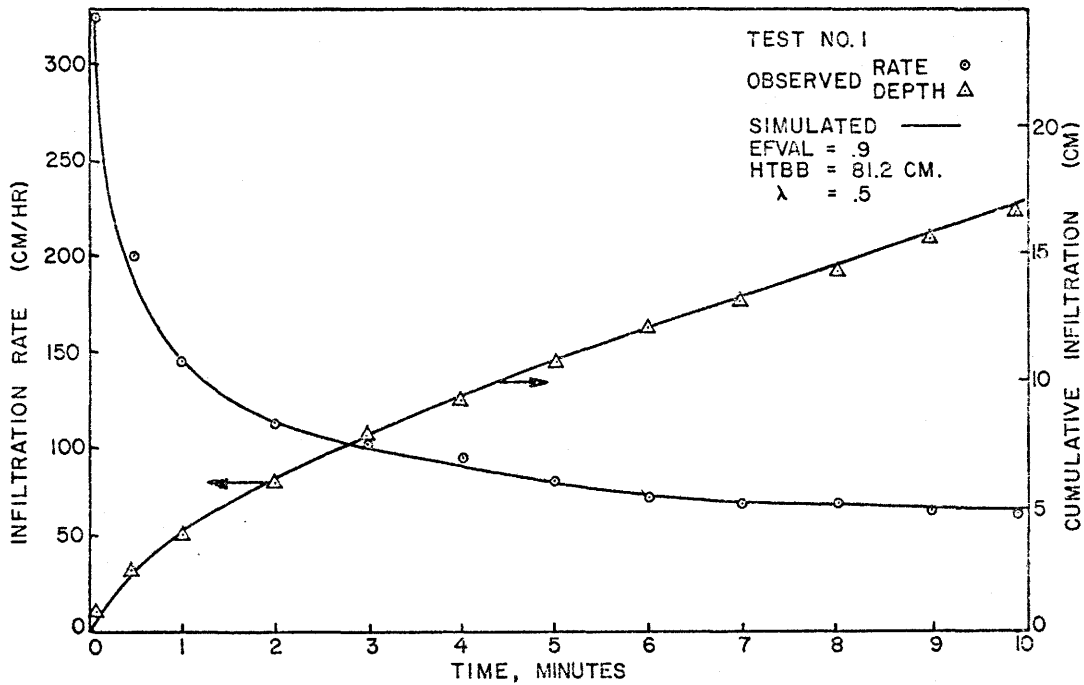


Figure 12. Observed and calculated infiltration curves for medium sandy loam.

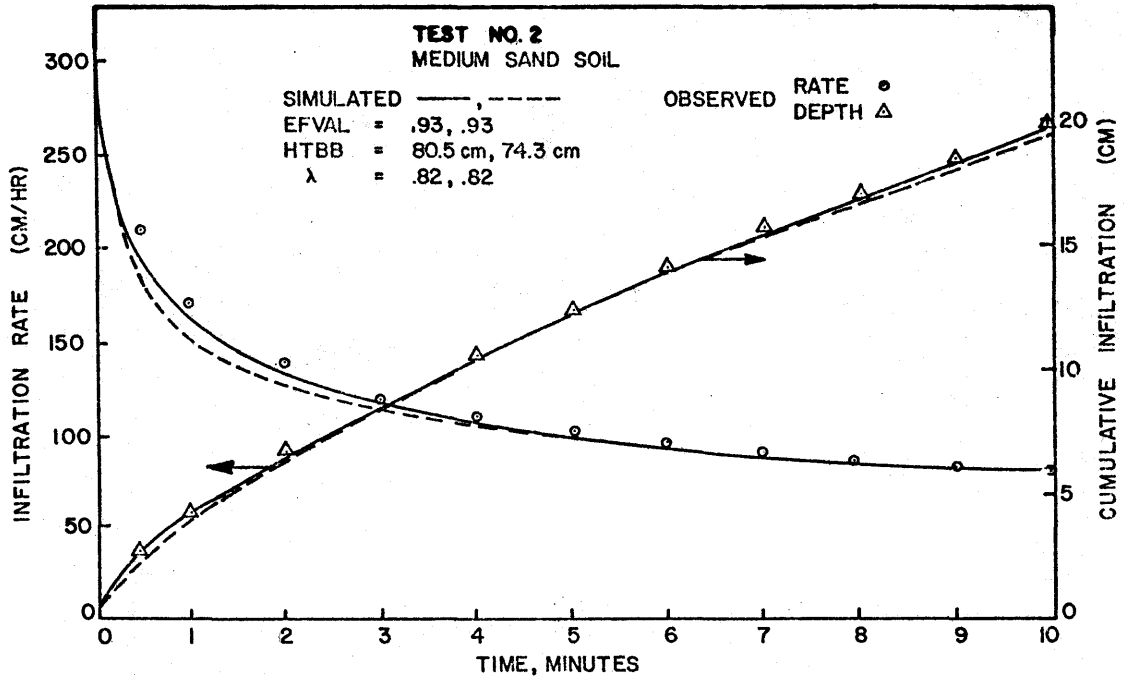


Figure 13. Observed and calculated infiltration curves for medium sandy soil.

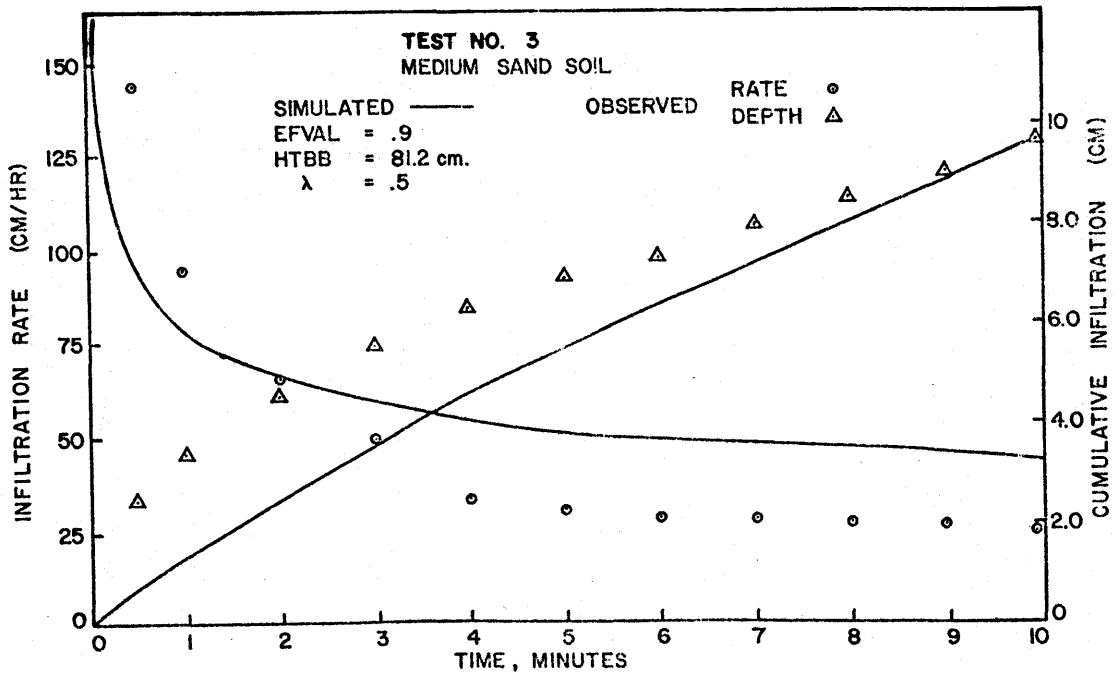


Figure 14. Observed and calculated infiltration curves for medium sandy soil.

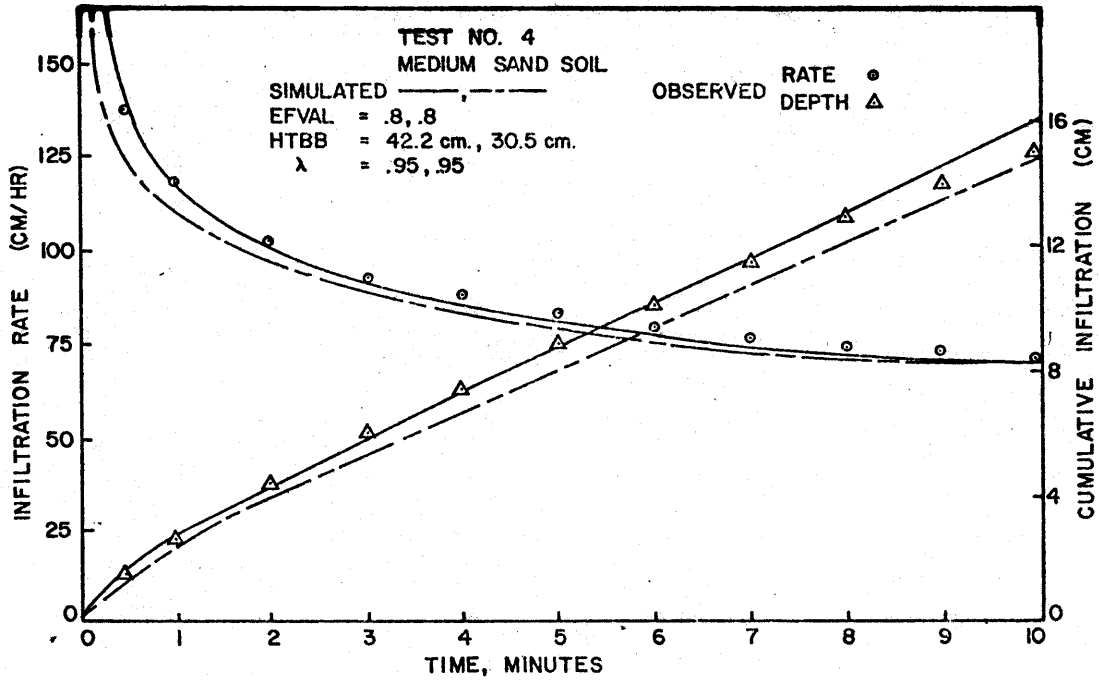


Figure 15. Observed and calculated infiltration curves for medium sandy soil.

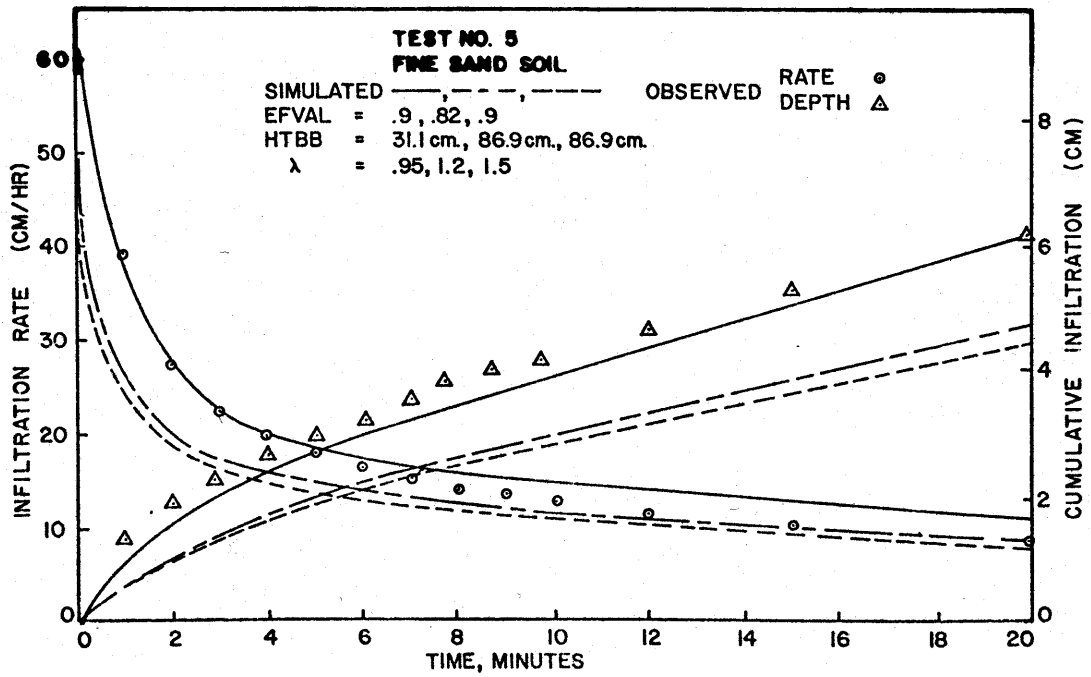


Figure 16. Observed and calculated infiltration curves for fine sandy soil.

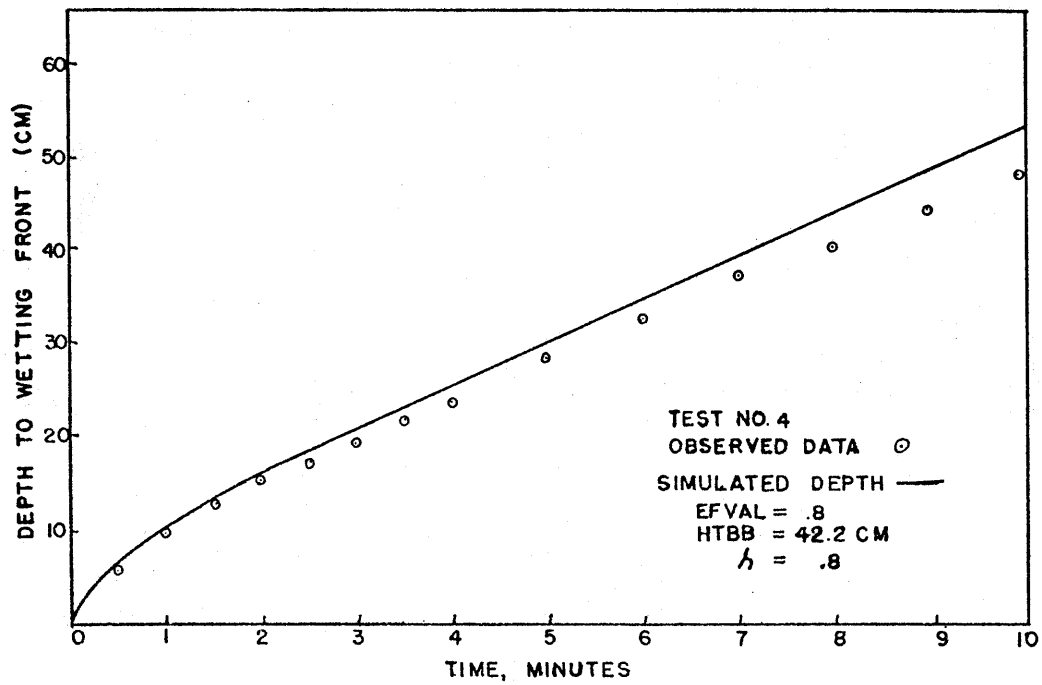


Figure 17. Wetting front movement for medium sandy soil.

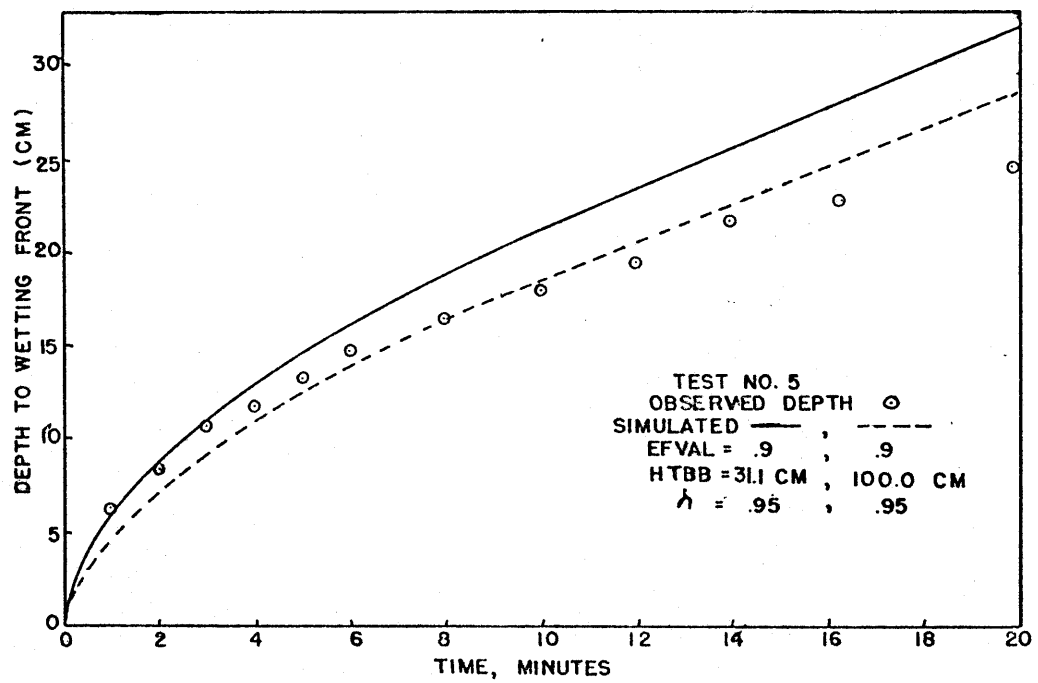


Figure 18. Wetting front movement for fine sandy soil.

$\theta(h)$ and $K(h)$ functions could be adjusted by visual observation of their effect on the agreement of the infiltration curves to the observed data.

Figure 19 shows the significance of the transition from the straight line equation of Brooks-Corey 29 to the curved line of King 31. This value controls the agreement of the infiltration rate curve with the observed data for long time periods, i.e., when the infiltration rate curve approaches the horizontal. If the transition value is too small, the curve will lie above the observed data, and conversely, if the transition value is too large, it will lie below the observed data.

The similarity of the curve to observed data for early times (i.e., when the curve is more nearly vertical) is controlled by the bubbling matric potential and the pore size distribution index λ , as shown in

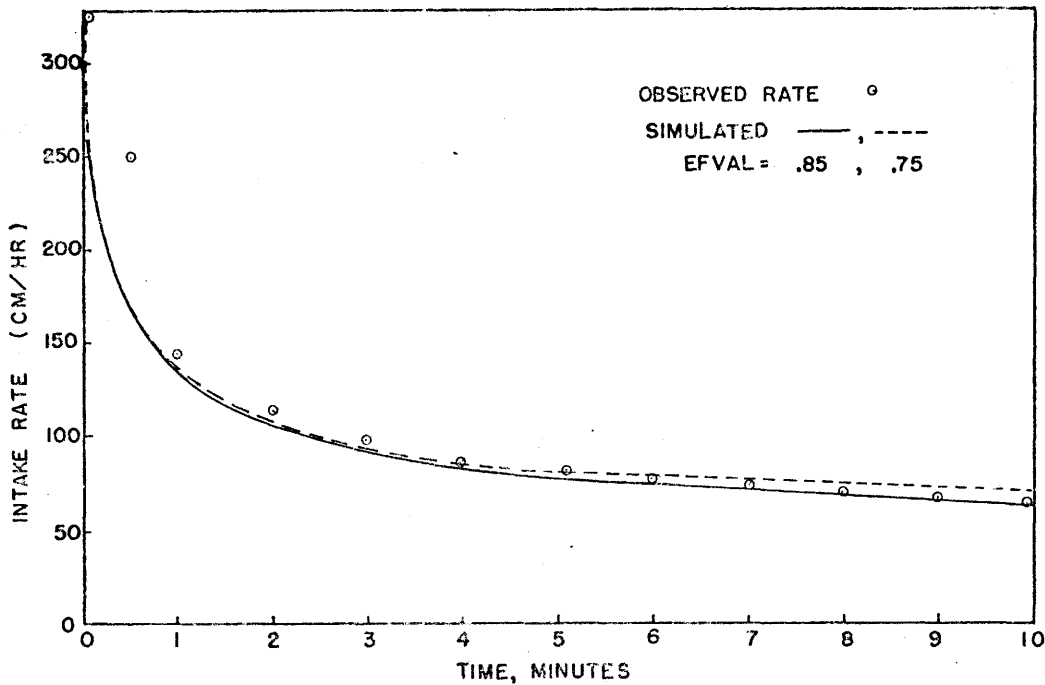


Figure 19. Effects of Brooks-Corey and King intercept on the infiltration curve.

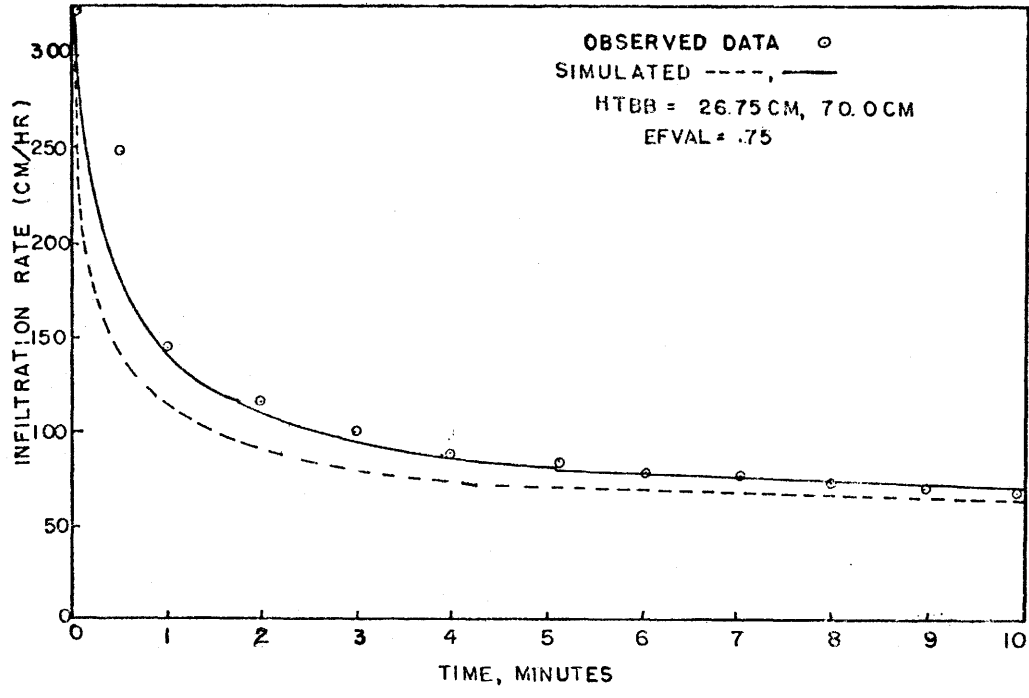


Figure 20. Effects of matrix bubbling potential on the infiltration curve.

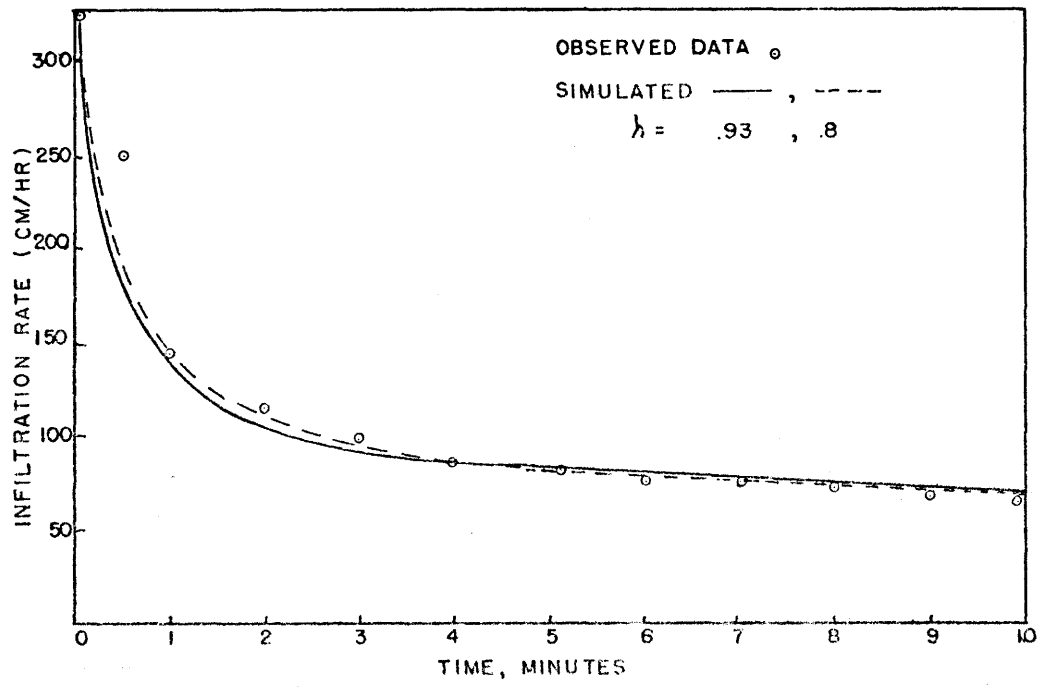


Figure 21. Effects of λ variation on the infiltration curve.

Figures 20 and 21. These two figures indicate the curve is more sensitive to the bubbling matric potential than the pore size distribution index λ . The computer program INFIL searched for the best fit of the curve to the observed data by varying the bubbling matric potential. If large differences in the agreement of the infiltration curve to the observed data are encountered, the pore size distribution index λ should be adjusted.

Observed $\theta(h)$ Relationships

The $\theta(h)$ relationship was determined for the medium-sand soil and fine-sand soil by the method discussed in Section IV. Figure 22 shows the agreement of the computer developed curve for effective saturation to the observed data. The data were obtained for this curve from sandy soil of the type used in tests 2-4. Figure 23 shows the agreement of the representative curve to the observed data for the soil used in test 5. It is possible to produce a very good representative curve of the $\theta(h)$ relationship by utilization of the proper parameters in the Brooks-Corey 29 and King 31 equations.

Reason for Discrepancies between Observed and Calculated Curves

The bubbling matric potential used by the computer to produce the best agreement of calculated infiltration rate-time curves to the observed rates vary from 42 cm for test 4 to 80 cm for test 2. These high values for the bubbling matric potential cause the most significant discrepancies between the observed and calculated infiltration rate-time curves at early times. The fitting of the observed and calculated curves at later times is rather insensitive to the bubbling matric

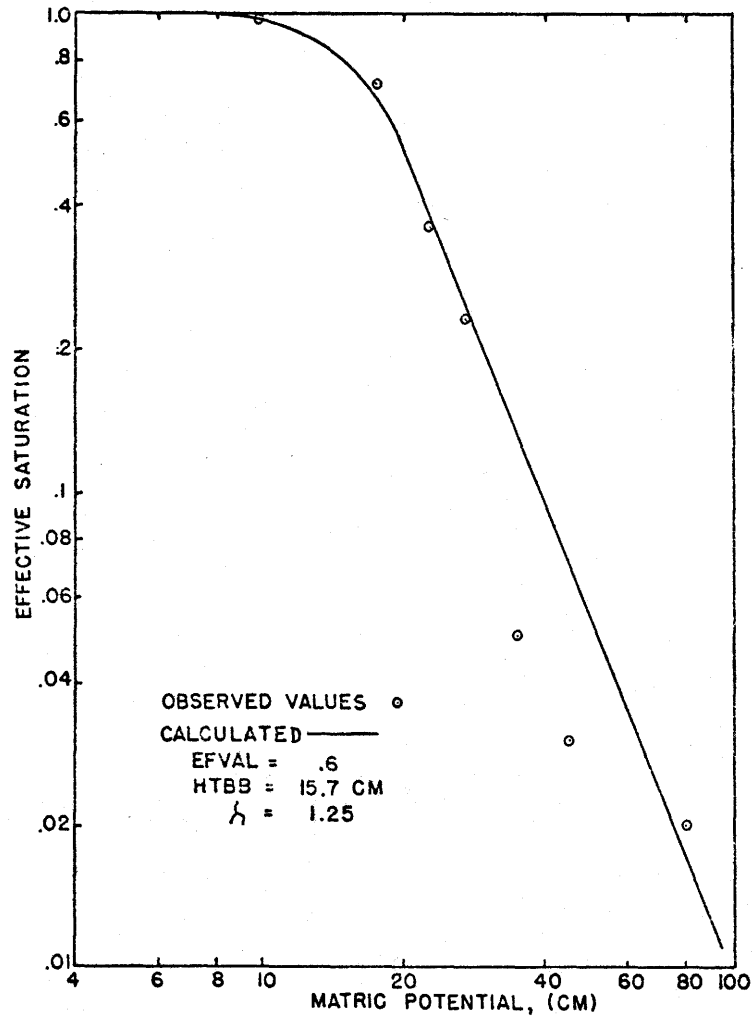


Figure 22. Effective saturation curve for tests 2-4.

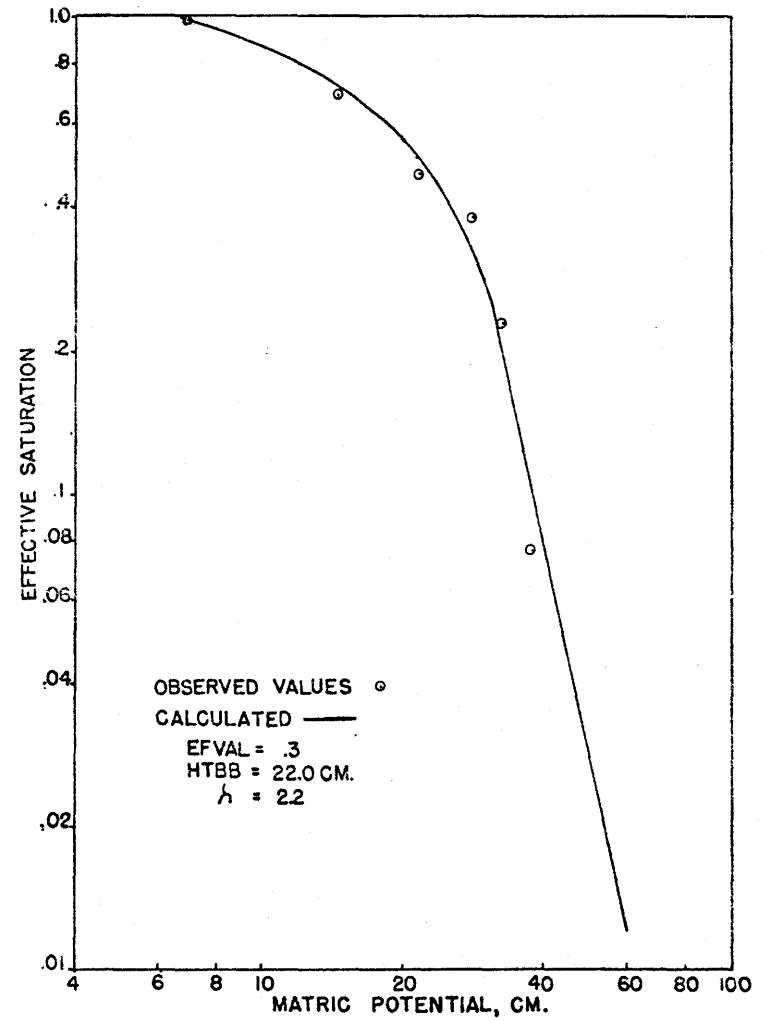


Figure 23. Effective saturation curve for test 5.

potential, since the bubbling matric potential could be reduced considerably without worsening the agreement for longer infiltration times. The process of infiltration at very early times may be dependent upon parameters other than those studied here. Also, obtaining accurate data from observations of the infiltration process at early times is extremely difficult without the aid of sensitive and expensive equipment.

The variation in the observed bubbling matric potentials of Figures 22 and 23 and that obtained from the calculated values used in INFIL, may be attributed to a number of problems encountered within an artificially packed soil, and the problems of modeling that soil. The sample used to determine data for Figures 22 and 23 contained about 26 grams of soil. After the sample was vacuum saturated, about 10 percent settlement in volume occurred in both samples. Since these samples were loaded at the same or nearly the same bulk density as the larger infiltration column, this decrease in volume would cause an increase in the bulk density of the sample. Work done by Laliberte, Corey and Brooks (1966) indicated that an increase in bulk density of a soil also increases the bubbling matric potential as well as λ . However, the results obtained from the observed and generated $\theta(h)$ curves indicate the opposite.

The problem of sample size must now be considered. The large columns showed a settlement factor of about 1 percent. This factor of settlement in the large columns could be omitted. Boundary effects on the smaller sample could introduce considerable variation in saturation. Along the container walls larger pores are encountered than

within the samples; since these pores may not become completely saturated their effect upon a small sample would affect the moisture characteristic curve considerably more than that of the larger column.

The variation of the bulk density within the columns as shown in Figure 24 must also be considered. The saturated hydraulic conductivity used in the computer program INFIL would only be valid for a particular layer of the most densely packed material. For more loosely packed areas the saturated hydraulic conductivity would be greater. The problem of nonhomogeneous soil within the column, when the computer solution assumes homogeneity, adds to the problem of poor agreement of observed and calculated infiltration curves.

The study of the infiltration process is a very complex undertaking. The movement of water into and through the soil matrix is affected by many factors. Among those which may influence agreement in the

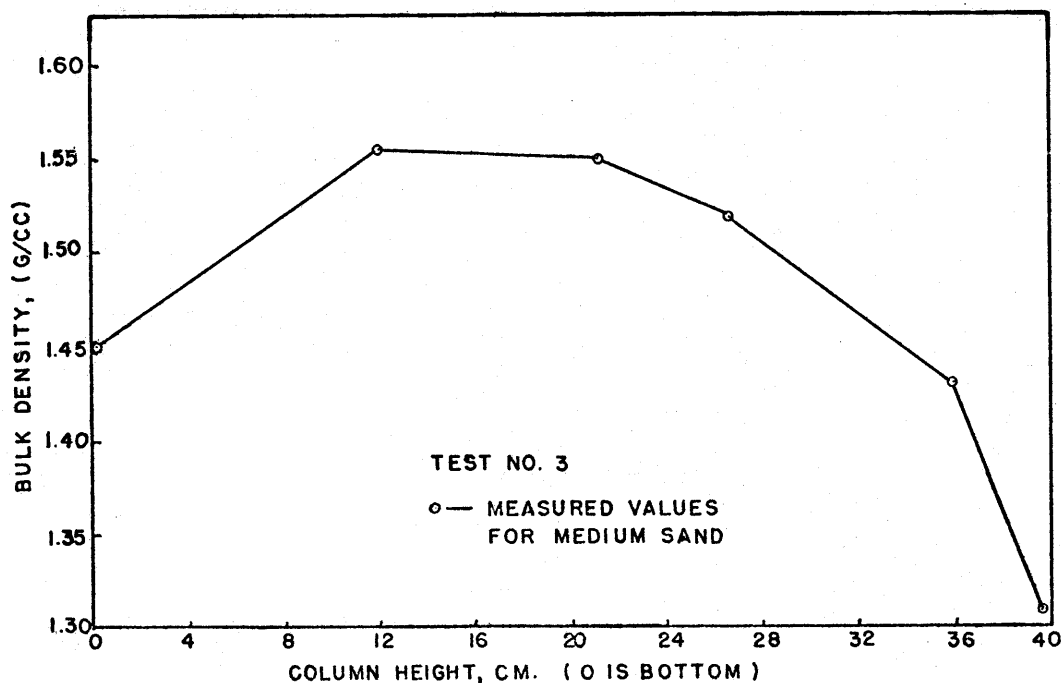


Figure 24. Variation of bulk density within the test column.

experimental work but which are not accounted for in the numerical solution are: (1) The air displaced by a rapidly advancing wetting front will not remain at atmospheric pressure as assumed in the development of the numerical solution. This phenomenon tends to retard the movement of the wetting front, thus decreasing the infiltration rate, especially at early times. (2) Darcy's Law may not be applicable to infiltration into sandy soils at early times. The upper limit of Darcy's Law, which is usually assumed to be equal to a Reynolds number of 1.0, may be exceeded if the flow velocity and mean pore diameter are large. (3) The percentage of entrapped air might have varied with depth in the soil columns owing to the variation in the rate of advance of the wetting front.

VI. SUMMARY AND CONCLUSIONS

Summary

A method for determining the water content - matric potential relationship and the hydraulic conductivity - matric potential relationship for infiltration into soil was developed and tested. A computer program INFIL, developed to solve the Richards equation numerically, applied these relationships as represented by equations of Brooks and Corey (1964) and King (1965) and simulated infiltration under various soil conditions.

The proposed method was evaluated by conducting a series of infiltration experiments with soil columns from which infiltration rate-time data were obtained. To apply the numerical solution it was also necessary to measure the initial and final soil water contents

and to estimate the hydraulic conductivity at the final water content. Then simulated infiltration tests were performed by the computer using various values of the parameters in the Brooks-Corey (1964) and King (1965) equations until the simulated infiltration rate-time relationship agreed closely with the observed infiltration rate-time data. These parameters included the bubbling matric potential, pore size distribution index, transition values on the $\theta(h)$ curve, and the hydraulic conductivity at the final water content. They were also determined from experimental tests and were found to be in satisfactory agreement with those selected by INFIL.

Conclusions

The primary conclusion is that the method proposed can be used to determine both the $\theta(h)$ and $K(h)$ relationships by numerical simulation of infiltration. The only data needed are the infiltration rate-time relationship, the initial and final water contents, and an estimate of the hydraulic conductivity at the final water content. This conclusion is based upon observations of infiltration into two types of sandy soil and from results of the observed values for the $\theta(h)$ relationships. It is possible to determine these relationships by the proposed method. Thus, extensive laboratory work involving conventional tests for determining these relationships can be eliminated.

Another conclusion is that for infiltration into field soils it is necessary to use both the Brooks-Corey (1964) and King (1965) relationships to adequately represent the $\theta(h)$ and $K(h)$ relationships. This conclusion is based upon the fact that the infiltration rates are sensitive to the θ and K values in those regions of the $\theta(h)$ and $K(h)$ curves where the matric potential is near the bubbling matric potential.

Recommendations for Future Study

The application of the proposed method of determining the $\theta(h)$ and $K(h)$ relationships of a soil under infiltration requires some additional work in order to attain the maximum potential value of the method. Some of this work is necessary to increase the range of applicability of the method, while other work would involve variation and improvement of the experimental methods and materials. The following areas should receive further study:

1. The program INFIL should be modified to include the hysteresis of the $\theta(h)$ and $K(h)$ relationships. Redistribution and drainage of soil water following the termination of infiltration could be simulated, and the soil moisture movement could be followed during an entire irrigation season on a day-to-day basis. This would allow an analysis of the effect of an irrigation management scheme on the amount of deep percolation, average daily water content, actual evapotranspiration, and water use efficiency.

2. Further development of the program INFIL should also be aimed at providing for the simulation of sprinkler irrigation or rainfall under either steady or time-varying application rates.

3. Similarly, the effect of crusting of the soil surface under the impact of large drops from sprinkler irrigation systems should be included in the program INFIL. As the surface crust develops, the $\theta(h)$ and $K(h)$ relationships applicable to it would change, resulting in redistribution of soil water below the crust. Alleviation of this crusting problem could be simulated by use of mulches, tillage practices, and smaller droplet sizes as a result of an increase in sprinkler pressure.

4. Infiltration into layered soils might also be simulated by a slight modification of the program INFIL. Since most soils in their natural state do exhibit some degree of layering, this step would increase the applicability of the proposed method to field conditions.

5. The use of gamma-ray equipment to measure the bulk density of the column without disturbing the sample should be included. This equipment could also be used to measure the initial and final moisture content, thus providing more precise information for use in INFIL. These measurements can be made not only in the laboratory but also in the field.

SELECTED REFERENCES

- Anat, A., H. R. Duke, and A. T. Corey. 1965. "Steady Upward Flow from Water Table." Hydrology Paper No. 7. Colo. State Univ., Fort Collins, Colorado.
- Bodman, G. B., and E. A. Coleman. 1944. "Moisture and Energy Conditions during Downward Entry of Water into Soils." Soil Sci. Soc. Amer. Proc. 8:116-122.
- Brooks, R. H., and A. T. Corey. 1964. "Hydraulic Properties of Porous Media." Hydrology Paper No. 3. Colo. State Univ., Fort Collins, Colorado.
- Buckingham, E. 1907. "Studies on the Movement of Soil Moisture." U.S.D.A. Bur. Soils Bull. No. 38.
- Childs, E. C. 1969. The Physics of Soil Water Phenomena. John Wiley and Sons, London. Pp. 153-294.
- Childs, E. C., and N. Collis-George. 1950. "The Permeability of Porous Materials." Proc. Roy. Soc. 201 A:392-405.
- Chow, V. T. (editor). 1964. Handbook of Applied Hydrology. McGraw-Hill, New York.
- Crank, J., and M. E. Henry. 1949. "Diffusion in Media with Variable Properties, I and II." Trans. Faraday Soc. 45:636-642, 1119-1128.
- Darcy, H. 1856. "Les Fontaines Publique de la Ville de Dijon." Dalmont, Paris.
- Gardner, W. R. 1958. "Some Steady State Solutions of the Unsaturated Moisture Flow Equations with Application to Evaporation from a Water Table." Soil Sci. 85:228-232.
- Gardner, W. R., and M. S. Mayhugh. 1958. "Solutions and Tests of the Diffusion Equation for the Movement of Water in Soil." Soil Sci. Soc. Amer. Proc. 22:197-201.
- Green, W. H., and G. A. Ampt. 1911. "Studies on Soil Physics, I: Flow of Air and Water through Soils." J. Agr. Sci. 4:1-24.
- Hagen, R. M., H. R. Haise and T. W. Edminister (editors). 1967. Irrigation of Agricultural Lands. Am. Soc. Agron., Madison, Wisconsin.

- Hanks, R. S., and S. B. Bowers. 1962. "Numerical Solution of the Moisture Flow Equation for Infiltration into Layered Soils." *Soil Sci. Soc. Amer. Proc.* 26:530-534.
- Holtan, H. N. 1961. "A Concept for Infiltration Estimates in Water Shed Engineering." *U.S.D.A. ARS* 41-51:25.
- Horton, R. E. 1940. "Approach toward a Physical Interpretation of Infiltration Capacity." *Soil Sci. Soc. Amer. Proc.* 5:339-417.
- King, L. G. 1965. "Description of Soil Characteristics for Partially Saturated Flow." *Soil Sci. Soc. Amer. Proc.* 29:359-362.
- Kirkham, D., and C. L. Feng. 1949. "Some Tests of the Diffusion Theory, and Laws of Capillary Flow, in Soils." *Soil Sci.* 67:29-40.
- Klute, A. 1952. "A Numerical Method for Solving the Flow Equation for Water in Unsaturated Materials." *Soil Sci.* 73:105-116.
- Kostiakov, A. N. 1932. "On the Dynamics of the Coefficient of Water Percolation in Soils and on the Necessity for Studying It from a Dynamic Point of View for Purposes of Amelioration." *Trans. Comm. Intern. Soil Sci. Soc., Moscow, 6th Part* A:17-21.
- Laliberte, G. E., A. T. Corey and R. H. Brooks. 1966. "Properties of Unsaturated Porous Media." *Hydrology Paper No. 17.* Colo. State Univ., Fort Collins, Colorado.
- Millington, R. J., and J. P. Quirk. 1959. "Permeability of Porous Media." *Nature* 183:387-388.
- Moore, R. E. 1939. "Water Conduction from Shallow Water Tables." *Hilgardia* 12:383-426.
- Peck, A. J. 1964. *Aust. J. Soil Res.* 2:1-7.
- Philip, J. R. 1957. "Numerical Solution of Equations of the Diffusion Type with Diffusivity Concentration-Dependent: 2." *Aust. J. Phys.* 10:29-42.
- Richards, L. A. 1931. "Capillary Conduction of Liquids through Porous Mediums." *Physics* 1:318-333.
- Richtmyer, R. D. 1957. Diffusion Methods for Initial Value Problems. Interscience Publ., New York.
- Rubin, J., and R. Steinhardt. 1963. "Soil Water Relations during Rain Infiltration, I: Theory." *Soil Sci. Soc. Amer. Proc.* 27:246-251.

- Skaggs, R. W., E. J. Monke, and L. F. Huggins. 1970. "An Approximate Method for Determining the Hydraulic Conductivity Function of Unsaturated Soil." Purdue Univ. WRRRC, Lafayette, Indiana, Tech. Rpt. No. 11.
- Swartzendruber, D. 1966. "Soil-Water Behavior as Described by Transport Coefficients and Functions." *Advan. Agron.* 18:327-370.
- Whistler, F. D., and A. Klute. 1966. "The Numerical Analysis of Infiltration, Considering Hysteresis, into a Vertical Soil Column at Equilibrium under Gravity." *Soil Sci. Soc. Amer. Proc.* 29:489-494.
- Young, E. G. 1957. *Soil Sci.* 84:283-290.

APPENDIX A

DERIVATION OF DIFFUSIVITY EQUATION
USED IN INFIL COMPUTER PROGRAM

The relationship developed by Brooks-Corey for relative hydraulic conductivity versus matric potential referred to earlier is

$$K_r = K_{sat} (-P_b / -P_c)^{\eta_1} , \quad (34)$$

where:

$$-P_b = -h_b / \gamma ,$$

$$-P_c = -h_c / \gamma .$$

Their relationship for effective saturation as a function of matric potential is

$$S_e = (-P_b / -P_c)^{\lambda_1} , \quad (29)$$

where:

$$S_e = (S - S_r) / (1 - S_r) , \quad (30)$$

as shown previously.

Equation 30 may be written as

$$S_e = (\theta - \theta_r) / (\theta_{sat} - \theta_r) , \quad (39)$$

where:

$$\theta = P \times S,$$

$$\theta_r = \text{residual water content determined by } P \times S_r,$$

θ_{sat} = porosity or maximum water content obtained immediately after infiltration.

The relationship 29 for effective saturation may be substituted into 32, resulting in

$$(P_b / -P_c)^{\lambda_1} = \frac{\theta - \theta_r}{\theta_{\text{sat}} - \theta_r} \quad , \quad (40)$$

and equation 40 may be written as

$$\theta = (\theta_{\text{sat}} - \theta_r) \times (-P_b)^{\lambda_1} \times (-P_c)^{-\lambda_1} + \theta_r \quad .$$

Water capacity is defined as

$$C(\theta) = \frac{d\theta}{dh} \quad . \quad (41)$$

Taking the derivative of 39 with respect to P_c produces

$$\begin{aligned} \frac{d\theta}{dP_c} &= (\theta_{\text{sat}} - \theta_r) (-P_b)^{\lambda_1} (-\lambda (-P_c)^{-\lambda_1-1}) \\ &= -\frac{\lambda_1 (\theta_{\text{sat}} - \theta_r)}{-P_c} [(-P_b) / (-P_c)]^{\lambda_1} \quad . \end{aligned} \quad (42)$$

Substituting equation 38 into equation 41 produces

$$C(\theta) = \frac{+\lambda_1 (\theta_{\text{sat}} - \theta_r)}{+P_c} \left(\frac{\theta - \theta_r}{\theta_{\text{sat}} - \theta_r} \right) \quad . \quad (43)$$

Equation 40 is solved for P_c next, as follows:

$$(-P_b / -P_c)^{\lambda_1} = \left(\frac{\theta - \theta_r}{\theta_{\text{sat}} - \theta_r} \right) \quad (44)$$

$$P_c = P_b \left(\frac{\theta - \theta_r}{\theta_{\text{sat}} - \theta_r} \right)^{-1/\lambda_1} \quad ,$$

and this relationship for P_c is substituted into equation 43, resulting in

$$C(\theta) = \frac{\lambda_1(\theta_{sat} - \theta_r)}{P_b \left(\frac{\theta - \theta_r}{\theta_{sat} - \theta_r} \right)^{-1/\lambda_1}} \times \left(\frac{\theta - \theta_r}{\theta_{sat} - \theta_r} \right),$$

or

$$C(\theta) = \frac{-\lambda_1(\theta_{sat} - \theta_r)}{P_b} \times \left(\frac{\theta - \theta_r}{\theta_{sat} - \theta_r} \right)^{1+\lambda_1}. \quad (45)$$

When η in the expression for the relative hydraulic conductivity 20 is replaced by $2 + 3\lambda_1$, the expression becomes

$$K_r = K_{sat} \times (-P_b / -P_c)^{2+3\lambda_1},$$

and substituting 40 into the above equation gives

$$K_r(\theta) = K_{sat} \times \left[\left(\frac{\theta - \theta_r}{\theta_{sat} - \theta_r} \right)^{1/\lambda_1} \right]^{2+3\lambda_1}. \quad (46)$$

Diffusivity is expressed as

$$D(\theta) = K(\theta) / C(\theta). \quad (6)$$

Equations 45 and 46 are substituted into equation 6, giving

$$D(\theta) = \frac{P_b \times K_{sat}}{\lambda_1} \times \left(\frac{\theta - \theta_r}{\theta_s - \theta_r} \right) \frac{1 + 2\lambda_1}{\lambda_1} \times (\theta_{sat} - \theta_r)^{-1},$$

and rearranging gives the diffusivity equation used in the INFIL computer program

$$D(\theta) = \frac{P_b \times K_{\text{sat}}}{\lambda_1} \times (\theta - \theta_r) \frac{1 + 2\lambda_1}{\lambda_1} \times (\theta_{\text{sat}} - \theta_r) \frac{-1 - 3\lambda_1}{\lambda_1}$$

(38)

APPENDIX B
COMPUTER PROGRAM INFIL

Included in this appendix are (1) list of variables used in INFIL program, (2) brief flow chart of program, (3) a listing and sample output from the INFIL program.

List of Variables Used in INFIL Program

- | | |
|--------|---|
| A | - coefficient 'A' defined in equation 23 (cm^2/sec). |
| AO | - value in RATE3, for unit intercept of infiltration curve on logarithmic plot. |
| A1 | - slope of logarithmic plot of INFIL curve. |
| ABSVOL | - area between measured and computed influx curves for one increment (cms). |
| ACCIF | - calculated accumulative infiltration (cm). |
| ADEA | - slope/2 of matric potential-hydraulic conductivity curve. |
| AL | - length of column studied (cm). |
| AMDA | - same as LAMDA. |
| APART | - deals with ACCIF and infiltration. |
| AW | - water content values X 1000., determines subscripts for use in RETEN. |
| B | - coefficient 'B' defined in equation 24. |
| BKS | - Brooks-Corey values for effective saturation. |
| C | - coefficient 'C' defined in equation 25. |
| CALVOL | - calculated volume developed by INFIL program (cm). |
| CLOCK | - experimental times from laboratory infiltration (min). |

- CRIT - minimum acceptable difference between values of water content assumed to define soil properties and the final water content obtained.
- D - coefficient 'D' defined in equation 26.
- DDT - increase in time increment computed after each time step (sec).
- DIFF - soil water diffusivity at each node point (cm²/sec).
- DP - values for diffusivities/4 used in solving of matrix.
- DT - time increments (seconds).
- DX - depth increment (cm).
- DY - diffusivity values calculated in RETEN from generated values of DIFF (cm²/sec).
- E - coefficient 'E' used in solving matrix.
- EFVAL - relative saturation value where deviation from st. line occurs.
- EXPI - measured infiltration rate (cm/hr).
- EXPART - difference between experimental values of volume at different time steps.
- EXPVOL - experimental volume values from laboratory infiltration (cm).
- F - coefficient 'F' used in solving matrix.
- H - matric potential (cm).
- HC - hydraulic conductivity (cm/sec).
- HDVAL - matric potential values in Brooks-Corey equation of saturation vs head giving effective saturation values of .5 (cm).
- HT - matric potential in Subroutine SETUP stored in array (cm).
- HTBB - matric bubbling potential (cm), approximated by the air entry value.
- HTBK - parameter in King equation similar to HTBB (cm).

HTN - generated matric potential values from SETUP (cm).

ITTER - number of iterations.

JJ - time step.

LAMDA - slope/2 of effective saturation vs matric potential curve.

NEX - number of infiltration rate-time data.

NI - number of depth increments.

NN - number of depth nodes.

NNCK - node point at which water content is continuously checked in short cut procedure.

NTRY - number of trials for minimum R value.

NVOL - number of EXPVOL data given.

P - porosity, or maximum water content immediately after infiltration

R - area between measured and calculated influx curves (cm).

RATE3 - calculated infiltration rate using fitted curve based on time and volume infiltrated (cm/hr).

RHCON - relative hydraulic conductivity.

SAT - saturation.

SATEF - effective saturation used in Brooks-Corey saturation vs. matric potential equation.

SATEFK - effective saturation constant used to determine King parameter HTBK.

SATK - saturated hydraulic conductivity (cm/sec).

THETR - residual water content based on residual saturation.
(cm^3/cm^3)

TIME - time (sec).

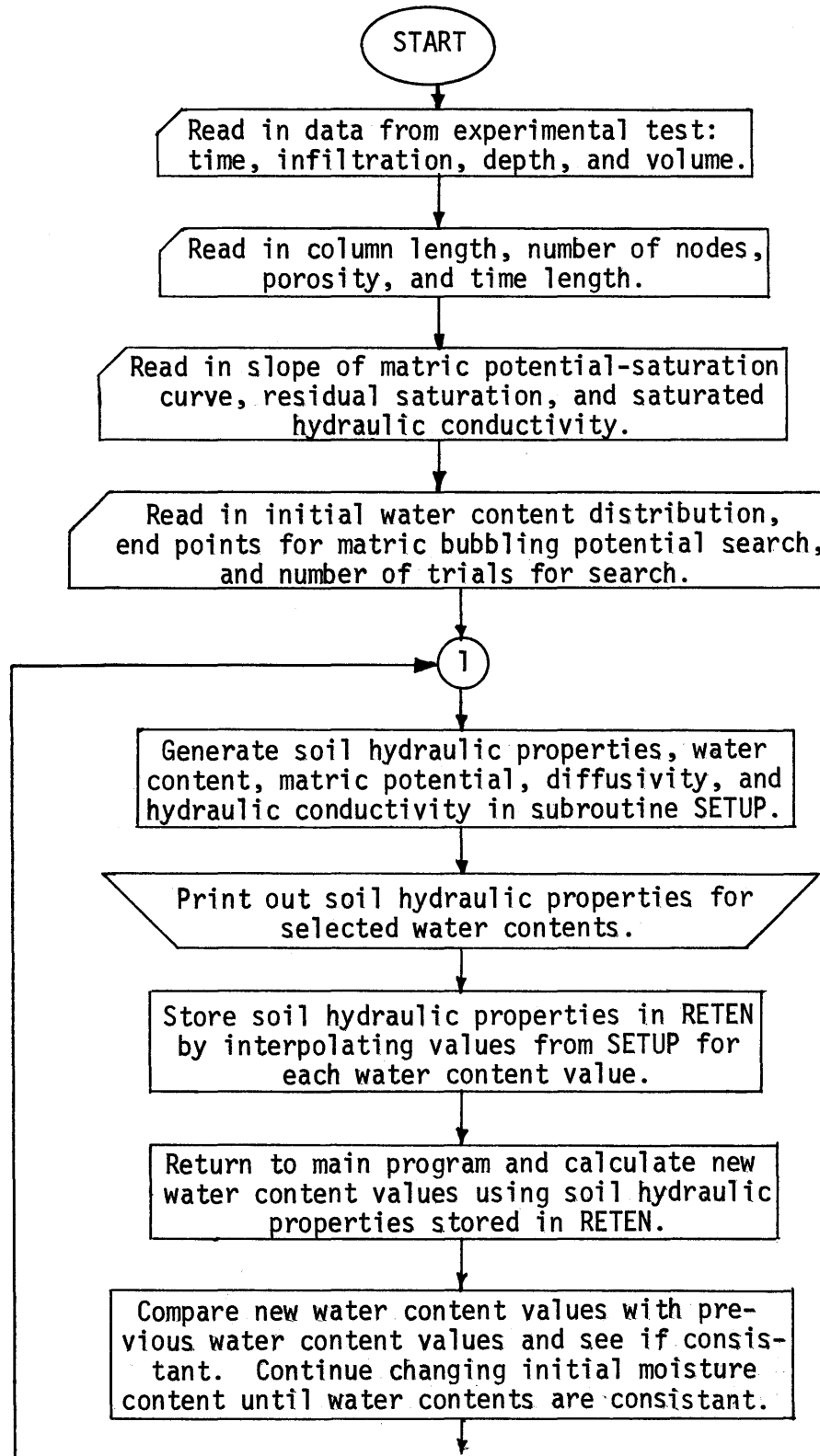
TMIN - time (minutes).

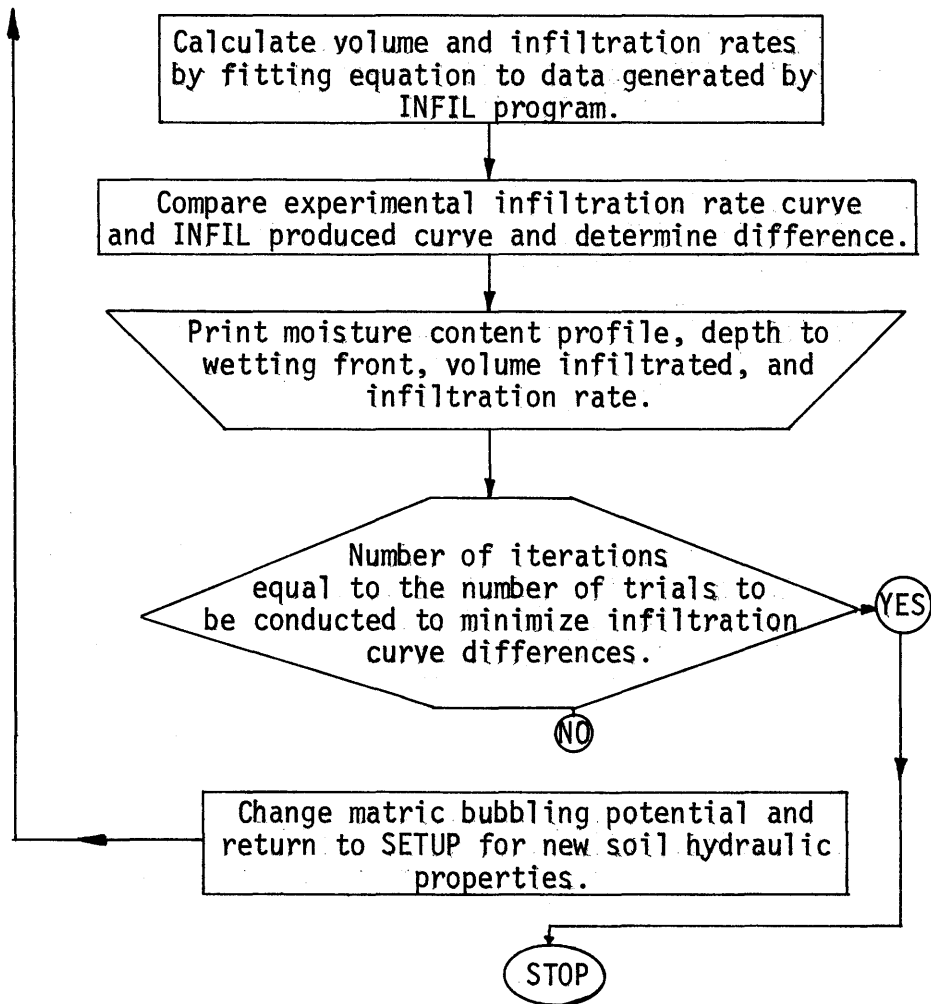
TSTOP - time at which solution is terminated (minutes).

U - slope of volume vs. time curve used to determine RATE3.

- WC - water content at nodes (cm^3/cm^3).
- WC1 - initial water content (cm^3/cm^3).
- WC2 - water content for previous iteration (cm^3/cm^3).
- WCC - water content initially, used to determine volume infiltrated (cm^3/cm^3).
- WCI - water content initially (cm^3/cm^3).
- WCN - generated water content developed in SETUP (cm^3/cm^3).
- WCT - tabular water contents stored in array for RETEN (cm^3/cm^3).
- WFL - depth to the wetting front (cm).
- XLONG - increment for which search is carried out to determine the correct HTBB (cm).
- XTRY - new trial value for optimum HTBB (cm).
- XXA, XXB - end points between which search is conducted for optimum HTBB (cm).

The following is a generalized flowchart for the INFIL computer program:






```

XTRY(1)=XXA+0.6180340*XLONG
XB=XTRY(KTRY)
HTBB = XTRY(KTRY)
IF (NTRY .EQ. 0) HTBB = XXA
35 CALL SETUP (SS1,AMDA,HTBB,SATRD,P,SATK)
PRINT 185
185 FORMAT (1H1)
ANI=NI
NN=NI+1
NT=NN
C DEFINE THE POSITION X
X(1)=0.0
DX =AL/ANI
CRIT = .001
NNCK=NN-5
DO 40 I=2,NN
IM=I-1
40 X(I)=X(IM)+DX
J=1
M=1
MP=2
WC(1,J) = WCI(J)
DO 45 I=2,NN
IF (Y(MP) .LT. X(I)) M = M + 1
MP=M+1
45 WC(I,J) = WCI(M) + (((X(I)-Y(M))/(Y(MP)-Y(M)))*(WCI(MP)-WCI(M)))
DO 50 I=1,NN
WC2(I) = WC(I,1)
WCC(I) = WC(I,1)
50 WC1(I)=WC(I,1)
IF (NN .GT. (NI+1)) NN=NI+1
C NOW THE INITIAL CONDITIONS HAVE BEEN EVALUATED. THE NEXT STEP
C IS TO EVALUATE THE COEFFICIENTS D AND K AT EACH NODE POINT.
DT = .001
C1=DT
JM=1
JJ=1
TMIN(1)=0.0
TIME=0.0
KK = 0
55 T(JJ)=TIME+DT
NIS=NN-1
L=1
CALL RETEN (J, NN, L, JJ, P)
KK = KK + 1
IF ( KK .EQ. 1 ) J = 2
TIME=T(JJ)
C TMIN REPRESENTS TIME IN MINUTES
TMIN(JJ)=T(JJ)/60.
60 DO 65 I=2,NIS
DX2DT=DX**2/DT
IP=I+1
IM=I-1
CP=(DIFF(IP,L)-DIFF(IM,L))*0.25
A(I)=DIFF(I,L)-DP
B(I)=-2.0*DIFF(I,L)-DX2DT
C(I)=DIFF(I,L)+DP
D(I)=0.50*DX*(FC(IP,L)-FC(IM,L))-WC(I,JM)*DX2DT
65 CCNTINUE
E(I)=0.0

```

```

F(1) = WC1(1)
DO 70 I=2,NIS
    IM=I-1
    DIVID=B(I)+A(I)*E(IM)
    E(I)=-C(I)/DIVID
70  F(I)=(D(I)-A(I)*F(IM))/DIVID
    WC(NN,J)=WC(NN,1)
    DO 75 I=1,NIS
        K=NN-I
        KP=NN-I+1
        WC(K,J)=F(K)+E(K)*WC(KP,J)
        IF ( WC(K,J) .LT. WCI(3) ) WC(K,J) = WCI(3)
        IF ( WC(K,J) .GT. P ) WC(K,J) = P
75  CONTINUE
C   WE NOW HAVE A DISTRIBUTION OF WC FOR THIS TIME STEP.
C   THE REDEFINITION OF DIFF(I) AND K(I) AND TESTING TO SEE IF
C   THE ORIGINAL ESTIMATE WAS SUFFICIENT FOLLOWS.
L=L+1
TRY =0.0
CALL RETEN (J,NN,L,JJ,P)
DO 80 I=1,NN
    IF (ABS(WC(I,J)-WC2(I)).GE. CRIT) TRY=1.
    WC2(I)=WC(I,J)
80  CONTINUE
C   IF THE SOLUTION HAS NOT CONVERGED AFTER 8 ITERATIONS, THE TIME
C   STEP IS REDUCED AND ANOTHER TRIAL IS MADE.
IF (L .GE. 8) GO TO 85
C   IF TRY=1, ANOTHER ITERATION WILL BE MADE.
IF (TRY .EQ. 1.0) GO TO 60
C   RATE1 IN CM/HR
C   ACCIF IN CM
C   ITTER=L-1
C   XI=ITTER
C   LOCATION OF WETTING FRONT
C   WFC-WETTING FRONT CONSTANT WFL-WETTING FRONT LOCATION(CM)
JM = (JJ + 2)/4
JK = JJ - 4 * JM
IF (JK .NE. 1) GO TO 88
WFC = ( P - WCI(3) ) * .1 + WCI(3)
DO 13 I = 2,NN
    IM = I - 1
    IF (WC(I,J) .LE. WFC) GO TO 14
13  CONTINUE
14  WFL(JJ) = ((WC(IM,J)-WFC)/(WC(IM,J)-WC(I,J)))*DX + X(IM)
    WRITE (1) (WC(I,J),I = 1,NT)
88  CALVOL(JJ) = 0.0
    DO 83 I = 1,NN
        CALVOL(JJ) = (WC(I,J) - WCC(I)) + CALVOL(JJ)
83  CONTINUE
    GO TO 90
C   THE FOLLOWING STATEMENTS REDUCE DT BY 1/2 FOR TIMES OF
C   NONCONVERGENCE.
C   *****
85  TIME=TIME-DT
    DT=DT/2.0
    GO TO 55
C   *****
90  CCNTINUE
    IF (TMIN(JJ) .GT. TSTOP) GO TO 105
    JJ=JJ+1

```

```

          DO 95 I=1,NN
            HC(I,1)=HC(I,L)
            DIFF(2,1)=DIFF(I,L)
95      THE FOLLOWING STATEMENTS IMPLEMENT A PART SCANNER FEATURE.
C      THIS MEANS THAT THE ENTIRE LENGTH OF THE COLUMN WILL NOT BE
C      CONSIDERED IN THE SOLUTION FOR ALL THE TIME.
C      *****
C      IF (ABS((WC(NNCK,J)-WC1(NNCK))/WC1(NNCK)) .GT. 0.001) NN=NN+5
C      IF (NN .GT. NT) NN=NT
C      DDT=5.0*(1.0-0.4*X1)
C      DT=DT+DDT
C      IF (DT .LE. 0.0) DT=D1
C      D1=DT
C      IF (JJ .EQ. 2) NN=NN/4
C      NNCK=NN-5
C      *****
C      IF (J .EQ. 1) GO TO 100
C      JM=2
C      J=1
100     GO TO 55
C      JM=1
C      J=2
105     GO TO 55
C      CONTINUE
C      REWIND 1
C      XSUM = 0.0
C      YSUM = 0.0
C      XSQ = 0.0
C      XYSUM = 0.0
C      JT = 0
C      DO 89 I = 1,JJ
C      V(I) = ALOG10(TMIN(I))
C      IF ( V(I) .LE. 0. ) GO TO 89
C      JT = JT + 1
C      Z(I) = ALOG10(CALVOL(I))
C      XSUM = V(I) + XSUM
C      YSUM = Z(I) + YSUM
C      XSQ = (V(I) *V(I)) + XSQ
C      XYSUM = V(I) * Z(I) + XYSUM
89     CONTINUE
C      XSUMSQ = XSUM * XSUM
C      AD = ((YSUM*XSQ) - (XSUM*XYSUM))/(JT*XSQ-XSUMSQ)
C      A1 = (JT*XYSUM-XSUM*YSUM)/(JT*XSQ - XSUMSQ)
C      U = 10.**AC
900    DO 900 I = 1,JJ
C      RATE3(I) = 60. * U * A1 * (TMIN(I) ** (A1 -1.))
C      DO 98 JI = 1,JJ
C      JM = (JI + 2)/4
C      JK = JI - 4*JM
C      IF (JK .NE. 1) GO TO 98
C      READ(1) (WC(I,J),I = 1,NT)
C      PRINT 195
195    FORMAT ( //,7X,'TIME      RATE      VOLUME WETTING',44X,
1      'WATER CONTENT' )
C      PRINT 200
200    FORMAT (4X,9H(MINUTES),1X,7H(CM/HR),3X,4H(CM),2X,'FRONT (CM)',6X,
1      '(X=0)',3X,'(X=1)',3X,'(X=2)',3X,'(X=3)',3X,'(X=4)',3X,'(X=5)',
2      3X,'(X=6)',3X,'(X=7)',3X,'(X=8)',2X,'(X=9)')
C      PRINT 190,TMIN(JI),RATE3(JI),CALVOL(JI),WFL(JI),(WC(I,J),I=1,10)
190    FORMAT ( /,3X,F8.2,2X,3F8.2,3X,10F8.3,/ )

```

```

106      II = 9
        II = II + 1
        KK = II + 9
        I = II + 1
        K = I + 9
        PRINT 191,II, KK, (WC(M,J), M = I,K)
191      FORMAT (10X, 'WATER CONTENT FROM', I3, '-', I2, 1X, 'CM', 3X, 10F8.3, /)
        IF (K .GE. NI) GO TO 193
        II = KK
        GO TO 106
193      CONTINUE
98      CCNTINUE
        REWIND 1
C      IF SEARCH IS NOT DESIRED, EXIT PROGRAM.
        IF (NEX .EQ. 0.0) GO TO 170
C      THE FOLLOWING SECTION EVALUATES THE ABSOLUTE DIFFERENCE
C      BETWEEN THE EXPERIMENTAL RATES AND THE PREDICTED RATES
C      AND DETERMINES THE NEXT TRIAL VALUE OF GH1.
C      *****
        ABSVOL(1)=0.0
        N=2
        TOTAL = CALVOL(1)
        DO 120 J=2,NEX
            DO 110 I=N,JJ
                IF (TMIN(I) .GE. CLOCK(J)) GO TO 115
110      CONTINUE
115      APART = CALVOL(I-1) - TOTAL
            APART=APART+(CLOCK(J)-TMIN(I-1))/(TMIN(I)-TMIN(I-1))*
                (CALVOL(I) - CALVOL(I-1))
            EXPART=EXPVOL(J)-EXPVOL(J-1)
            ABSVOL(J)=ABS(EXPART-APART)
            TOTAL=TOTAL+APART
            N=I
            IF ( TMIN(I) .GE. TSTOP ) GO TO 121
120      CONTINUE
121      SUM=0.0
            DO 125 K=1,NEX
125      SUM=SUM+ABSVOL(K)
            PRINT 235, SUM
235      FORMAT (1H0/1H0,15X,36HTHE ABSOLUTE DIFFERENCE BETWEEN THE /16X,5
1      HCALCULATED AND EXPERIMENTAL INFILTRATION CURVES IS , F10.4)
            SS1=1.0
            R(KTRY)=SUM
            IF (KTRY .EQ. 1) GO TO 130
            GO TO 135
130      XTRY(2)= XXA+XXB-XB
            KTRY=KTRY+1
            RSMALL=R(1)
            HTBB = XTRY(KTRY)
            GO TO 35
135      IF (R(KTRY) .LT. RSMALL) GO TO 145
            IF (XTRY(KTRY) .GT. XB) GO TO 140
            XXA=XTRY(KTRY)
            GO TO 160
140      XXB=XTRY(KTRY)
            GO TO 160
145      RSMALL=R(KTRY)
            IF (XTRY(KTRY) .GT. XB) GO TO 150
            XXB=XB
            GO TO 155

```

```

150   XXA=XB
155   XB=XTRY(KTRY)
160   IF (KTRY .GE. NTRY) GO TO 165
      KTRY=KTRY+1
      XTRY(KTRY)=XXA+XXB-XB
      HTBB_ = XTRY(KTRY)
      GO TO 35
C     *****
165   PRINT 245, (XTRY(I),          R(I), I=1,NTRY)
245   FORMAT (2F20.4)
170   CONTINUE
      STOP
      END

```

```

      SUBROUTINE RETEN (J,NN,L,JJ,P)
C
C     THIS SUBROUTINE CONVERTS W ARRAY TO CORRESPONDING
C     H, DIFF, AND K ARRAYS.
C
      COMMON      HT(750),HCT(750), H(750), WC1(125), WCI(125),Y(25)
1     ,X(125), A(125), B(125), C(125), C(125), E(125), F(125),DY(750),
3     WCC(125), WC(125,2), HC(125,10), DIFF(125,10),T( 800),RATE3( 800
4     ), TMIN( 800), CALVOL(800), WC2(125),          XTRY(25),WFL( 800)
      DO 5 I=1,NN
      AW = WC(I,J) * 1000.000 + .CC1
      IW=AW
1     BW=IW
      IWP=IW+1
2     COEFF=AW-BW
      H(I) = HT(IW)
      DIFF(I,L) = DY(IW)
      HC(I,L) = HCT(IW)
      IF (WC(I,J) .GE. P) GO TO 5
3     H(I)= HT(IW)+COEFF*( HT(IWP)- HT(IW))
4     DIFF(I,L)=DY(IW)+COEFF*(DY(IWP)-DY(IW))
6     HC(I,L) = HCT(IW) + COEFF * (HCT(IWP) - HCT(IW))
5     CONTINUE
      RETURN
      END

```

SUBROUTINE SETUP (SS1,AMCA,HTBB,SATRC,P,SATK)

C THIS SUBROUTINE USES THE SOIL PARAMETERS, LAMDA, PB, SR, N, KSAT. NND
 C UTILIZES THE BROOKS-COREY EQUATIONS OF EFFECTIVE SATURATION VS CAPILLARY
 C PRESSURE AND HYDRAULIC CONDUCTIVITY VS CAPILLARY PRESSURE TO DETERMINE
 C THE HYDRAULIC CONDUCTIVITY FOR KNOWN MOISTURE CONTENTS.

 C LISTING OF SYMBOLS USED IN THE PROGRAM
 C SATEF - EFFECTIVE SATURATION WCT-WATER CONTENT
 C AMDA - LAMDA (SLOPE OF EFFECTIVE SATURATION-CAPILLARY PRESS. CURVE
 C SAT - SATURATION SATRC - RESIDUAL SATURATION PRTY - POROSITY
 C HT - CAPILLARY PRESSURE HTBB - BUBBLING PRESSURE
 C RHCON - RELATIVE HYDRAULIC COND. SATK - SATURATED HYDRAULIC COND
 C HCT - HYDRAULIC CONDUCTIVITY HT - HEAD WITHOUT INTERPOLATION
 COMMON HT(750),HCT(750), H(750), WC1(125), WCI(125),Y(25)
 1 ,X(125), A(125), B(125), C(125), D(125), E(125), F(125),DY(750),
 3 WCC(125), WC(125,2), HC(125,10), DIFF(125,10),T(800),RATE3(800
 4), TMIN(800), CALVOL(800), WC2(125), XTRY(25),WFL(800)
 DIMENSION RHCON(750),HTN(750),WCN(750),SATEF(720),WCT(750)
 IF (SS1 .GT. 0.0) GO TO 25
 TAMDA = 2. * AMDA
 ADEA = 1. + 3.*AMDA
 TADEA = 2. * ADEA
 HTN(1) = 0.0
 KK = 1
 DO 801 L = 1,5
 LI = L - 1
 DO 801 K = 2,19
 AK = K
 BK = AK/20.
 KK = KK + 1.
 HTN(KK) = BK*10.**LI
 IF (HTN(KK) .GE. 1500.) GO TO 800
 801 CONTINUE
 800 CONTINUE
 25 CCNTINUE
 SATEF(1) = 1.0
 WCN(1) = P
 EFVAL = .90
 HDVAL = HTBB*(EFVAL ** (1./(-TAMDA)))
 HTBK = HTBB
 BOT = HTBK
 DO 880 M = 1,500
 FACT = (HDVAL/HTBK)**(-AMDA)
 SATEFK = (COSH(FACT) - 1.) / (COSH(FACT) + 1.)
 IF (ABS (SATEFK - EFVAL) .LE. .005) GO TO 881
 IF (SATEFK - EFVAL) 6,881,4
 4 HTBK = (BOT + HTBK) / 2.C
 GO TO 880
 6 BOT = HTBK
 HTBK = HTBK + 2.J
 880 CCNTINUE
 881 KL = 0
 KN = 2
 RH = ((HDVAL/HTBB) **(-TADEA))
 HTBK1 = HTBK
 BOT1 = HTBK1
 DO 100 N = 1,500

```

FAT = ( HDVAL/HTBK1 ) ** ( -ADEA )
RHCONK = ( COSH(FAT) - 1. ) / ( COSH(FAT) + 1. )
IF ( ABS (RHCONK-RH) .LE. .005 ) GO TO 32
IF ( RHCCNK - RH ) 7,32,5
5 HTBK1 = (BOT1 + HTBK1 )/2.0
GO TO 100
7 ROT1 = HTBK1
HTBK1 = HTBK1 + 2.0
100 CCNTINUE
32 THETR = .001
DO 802 KY = 2, KK
BKS = (HTN(KY)/HTBB)**(-TAMCA)
IF ( KL .EQ. 1 ) GO TO 790
FACT1 = (HTN(KY)/HTBK)**(-AMDCA)
SATEF(KY) = 1.0
IF ( FACT1 .GT. 170. ) GO TO 789
SATEF(KY) = (COSH(FACT1) - 1.)/(COSH(FACT1)+1.)
789 CONK = SATEF(KY)
IF ( BKS .GT. SATEF(KY) ) GO TO 808
790 SATEF(KY) = BKS
KL = 1
808 SAT = (1. - SATRD ) * SATEF(KY) + SATRD
WCN(KY) = P * SAT
IF ( WCN(KY) .LT. WCI(3)) GO TO 399
KN = KN + 1
CONTINUE
802 IP = P * 1000. + .5
399 IPM = IP - 1.
AB = WCI(3) * 1000. + .5
IB = AB - 1
J = 1
DO 803 KT = IB, IPM
AKT = KT/1000.
DO 804 KA = J, KN
K1 = KN + 1 - KA
IF ( AKT .LT. WCN(K1)) GO TO 805
804 CONTINUE
805 J = KA
HT(KT) = HTN(K1) + ((WCN(K1)-AKT)/(WCN(K1)-WCN(K1+1))) *
1 (ABS(HTN(K1) - HTN(K1+1)))
HT(KT) = -(HT(KT))
803 CONTINUE
HT(IP) = 0.0
PRINT 40
40 FORMAT (2H1 )
PRINT 45 ,AMDCA,ADEA,HTBB,SATRD
45 FORMAT ( 21X, 'LAMDA = ', F5.3, 3X, 'ADEA = ', F6.3,/, 21X,
1 'BUBBLING PRESSURE = ', F5.2, ' RESIDUAL SATURATION = ', F5.3)
DTHET = P - THETR
DTHETP = DTHET ** (-((1. + 3. * TAMDA )/ TAMDA))
PWR = ((1. + 2. *(TAMCA))/(TAMCA))
DO 806 I = IB, IPM
SATEF(I) = (HT(I)/(-HTBB))**(-TAMDA)
RHCCN(I) = ((HT(I)/(-HTBB)) **(-TACEA ))
IF ( SATEF(I) .LT. CONK ) GO TO 71
FACT3 = ((HT(I)/(-HTBK))**(-AMDCA))
SATEF(I) = (COSH(FACT3) - 1. ) / (COSH(FACT3) + 1. )
71 IF ( RHCCN(I) .LT. RH ) GO TO 807
FACT2 = ((HT(I)/(-HTBK1))**(-ADEA))
RHCON(I) = 1.0

```

```

      IF ( FAC12 .GT. 170. ) GO TO 807
      RHCCN(I) = (COSH(FACT2) - 1.0 ) / ( COSH(FACT2) + 1.0 )
807  SAT = ( 1. - SATRD ) * SATEF(I) + SATRD
      WCT(I) = P * SAT
806  HCT(I) = RHCON(I) * SATK
      WCT(IP) = P
      DO 870 M = IB,IP
870  DY(M) = (HTBB*SATK/(TAMDA))*DTHETP*((WCT(M)-THETR)**PWR )
      HCT(IP) = SATK
      PRINT 70
70  FORMAT (1H0/1H0)
      PRINT 75
75  FORMAT (28X, 24HTABLE OF SOIL PROPERTIES )
      PRINT 80
80  FORMAT (1H0/1H0/25X,4HHEAD,17X,5HTHETA,12X,12HCONDUCTIVITY,7X,
1  'DIFFUSIVITY' )
      PRINT 65
65  FORMAT ( 1H /25X,'(CM)',15X,'(PERCENT)',12X,'(CM/SEC)',9X,
1  '(CM**2/SEC)' )
      PRINT 70
      DO 810 J = IB,IP,10
      PRINT 810, HT(J),WCT(J),HCT(J),DY(J)
810  FORMAT ( 12X, 4E20.5 )
      PRINT 810, HT(IP),WCT(IP),HCT(IP),CY(IP)
      RETURN
      END

```

EXPERIMENTAL DATA

TIME (MINUTES)	RATE (CM/HR)	VOLUME (CM)
.00	2000.00	.00
.50	138.00	1.48
1.00	119.30	2.53
2.00	102.00	4.40
3.00	93.00	6.00
4.00	88.00	7.50
5.00	83.50	8.90
6.00	80.00	10.10
7.00	77.00	11.50
8.00	75.00	12.70
9.00	74.00	14.00
10.00	72.00	15.00

INPUT DATA FOR INFIL

AL = 60.0 , NI = 60, P = .36, tstop = 30.0	WCI	Y
	.36	0.0
amda = .95, satrd = .02, satk = 2.25 x 10 ⁻²	.02	.1
	.02	60.0
XXA = 75., XXB = 100., NTRY = 4		

LAMDA = .950 ADEA = 3.850
 BUBBLING PRESSURE = 30.45 RESIDUAL SATURATION = .020

TABLE OF SOIL PROPERTIES

HEAD (CM)	THETA (PERCENT)	CONDUCTIVITY (CM/SEC)	DIFFUSIVITY (CM**2/SEC)
-.18658E+03	.18465E-01	.19512E-07	.11156E-03
-.13801E+03	.27178E-01	.19891E-06	.58009E-03
-.11274E+03	.36536E-01	.94364E-06	.16562E-02
-.93652E+02	.48933E-01	.39374E-05	.42359E-02
-.83672E+02	.58897E-01	.93763E-05	.74361E-02
-.76255E+02	.68868E-01	.19162E-04	.11782E-01
-.70425E+02	.78928E-01	.35352E-04	.17444E-01
-.65788E+02	.88838E-01	.59730E-04	.24381E-01
-.61985E+02	.98615E-01	.94465E-04	.32644E-01
-.58698E+02	.10859E+00	.14371E-03	.42615E-01
-.55838E+02	.11868E+00	.21112E-03	.54386E-01
-.53448E+02	.12834E+00	.29568E-03	.67315E-01
-.51253E+02	.13839E+00	.40839E-03	.82567E-01
-.49296E+02	.14846E+00	.55115E-03	.99784E-01
-.47655E+02	.15785E+00	.71526E-03	.11763E+00
-.46014E+02	.16822E+00	.93675E-03	.13944E+00
-.44547E+02	.17844E+00	.12023E-02	.16319E+00
-.43360E+02	.18746E+00	.14801E-02	.18602E+00
-.42173E+02	.19722E+00	.18327E-02	.21281E+00
-.40987E+02	.20781E+00	.22833E-02	.24437E+00
-.39861E+02	.21871E+00	.28293E-02	.27964E+00
-.39037E+02	.22727E+00	.33230E-02	.30939E+00
-.38213E+02	.23637E+00	.39162E-02	.34304E+00
-.37389E+02	.24607E+00	.46320E-02	.38119E+00
-.36565E+02	.25640E+00	.54991E-02	.42456E+00
-.35741E+02	.26743E+00	.65540E-02	.47401E+00
-.34844E+02	.28030E+00	.79708E-02	.53596E+00
-.33295E+02	.29407E+00	.10552E-01	.60736E+00
-.31746E+02	.30179E+00	.13148E-01	.64978E+00
-.30197E+02	.30933E+00	.15870E-01	.69290E+00
-.28018E+02	.31949E+00	.19288E-01	.75366E+00
-.25746E+02	.32929E+00	.21532E-01	.81520E+00
-.22951E+02	.33983E+00	.22420E-01	.88472E+00
-.19811E+02	.34914E+00	.22500E-01	.94896E+00
-.11810E+02	.35949E+00	.22500E-01	.10236E+01
.00000E+00	.36000E+00	.22500E-01	.10274E+01

TIME (MINUTES)	RATE (CM/HR)	VOLUME (CM)	WETTING FRONT (CM)	WATER CONTENT										
				(X=0)	(X=1)	(X=2)	(X=3)	(X=4)	(X=5)	(X=6)	(X=7)	(X=8)	(X=9)	
.00	858.69	.00	.78	.360	.020	.020	.020	.020	.020	.020	.020	.020	.020	.020
				.020	.020	.020	.020	.020	.020	.020	.020	.020	.020	.020
				.020	.020	.020	.020	.020	.020	.020	.020	.020	.020	.020
				.020	.020	.020	.020	.020	.020	.020	.020	.020	.020	.020
				.020	.020	.020	.020	.020	.020	.020	.020	.020	.020	.020
				.020	.020	.020	.020	.020	.020	.020	.020	.020	.020	.020

TIME (MINUTES)	RATE (CM/HR)	VOLUME (CM)	WETTING FRONT (CM)	WATER CONTENT										
				(X=0)	(X=1)	(X=2)	(X=3)	(X=4)	(X=5)	(X=6)	(X=7)	(X=8)	(X=9)	
.15	153.34	.64	3.30	.360	.320	.255	.125	.024	.020	.020	.020	.020	.020	.020
				.020	.020	.020	.020	.020	.020	.020	.020	.020	.020	.020
				.020	.020	.020	.020	.020	.020	.020	.020	.020	.020	.020
				.020	.020	.020	.020	.020	.020	.020	.020	.020	.020	.020
				.020	.020	.020	.020	.020	.020	.020	.020	.020	.020	.020
				.020	.020	.020	.020	.020	.020	.020	.020	.020	.020	.020

TIME (MINUTES)	RATE (CM/HR)	VOLUME (CM)	WETTING FRONT (CM)	WATER CONTENT										
				(X=0)	(X=1)	(X=2)	(X=3)	(X=4)	(X=5)	(X=6)	(X=7)	(X=8)	(X=9)	
.18	147.63	.74	3.59	.360	.328	.278	.183	.034	.020	.020	.020	.020	.020	.020
				.020	.020	.020	.020	.020	.020	.020	.020	.020	.020	.020
				.020	.020	.020	.020	.020	.020	.020	.020	.020	.020	.020
				.020	.020	.020	.020	.020	.020	.020	.020	.020	.020	.020
				.020	.020	.020	.020	.020	.020	.020	.020	.020	.020	.020
				.020	.020	.020	.020	.020	.020	.020	.020	.020	.020	.020

TIME (MINUTES)	RATE (CM/HR)	VOLUME (CM)	WETTING FRONT (CM)	WATER CONTENT									
				(X=0)	(X=1)	(X=2)	(X=3)	(X=4)	(X=5)	(X=6)	(X=7)	(X=8)	(X=9)
9.80	69.54	14.32	46.77	.360	.359	.358	.357	.356	.355	.354	.353	.352	.351
WATER CONTENT FROM 10-19 CM				.350	.349	.348	.348	.347	.346	.345	.344	.343	.342
WATER CONTENT FROM 20-29 CM				.342	.341	.340	.339	.338	.338	.337	.336	.335	.334
WATER CONTENT FROM 30-39 CM				.334	.333	.332	.330	.329	.328	.326	.324	.322	.319
WATER CONTENT FROM 40-49 CM				.315	.308	.298	.284	.261	.228	.177	.070	.020	.020
WATER CONTENT FROM 50-59 CM				.020	.020	.020	.020	.020	.020	.020	.020	.020	.020

TIME (MINUTES)	RATE (CM/HR)	VOLUME (CM)	WETTING FRONT (CM)	WATER CONTENT									
				(X=0)	(X=1)	(X=2)	(X=3)	(X=4)	(X=5)	(X=6)	(X=7)	(X=8)	(X=9)
9.87	69.45	14.41	47.13	.360	.359	.358	.357	.356	.355	.354	.353	.352	.351
WATER CONTENT FROM 10-19 CM				.350	.349	.349	.348	.347	.346	.345	.344	.343	.342
WATER CONTENT FROM 20-29 CM				.342	.341	.340	.339	.339	.338	.337	.336	.335	.335
WATER CONTENT FROM 30-39 CM				.334	.333	.332	.331	.330	.328	.327	.325	.323	.320
WATER CONTENT FROM 40-49 CM				.316	.310	.301	.288	.268	.238	.193	.105	.023	.020
WATER CONTENT FROM 50-59 CM				.020	.020	.020	.020	.020	.020	.020	.020	.020	.020

TIME (MINUTES)	RATE (CM/HR)	VOLUME (CM)	WETTING FRONT (CM)	WATER CONTENT									
				(X=0)	(X=1)	(X=2)	(X=3)	(X=4)	(X=5)	(X=6)	(X=7)	(X=8)	(X=9)
9.97	69.32	14.54	47.51	.360	.359	.358	.357	.356	.355	.354	.353	.352	.351
WATER CONTENT FROM 10-19 CM				.351	.350	.349	.348	.347	.346	.345	.344	.343	.343
WATER CONTENT FROM 20-29 CM				.342	.341	.340	.339	.339	.338	.337	.336	.336	.335
WATER CONTENT FROM 30-39 CM				.334	.333	.332	.331	.330	.329	.327	.326	.324	.321
WATER CONTENT FROM 40-49 CM				.318	.313	.305	.294	.277	.251	.213	.153	.040	.020
WATER CONTENT FROM 50-59 CM				.020	.020	.020	.020	.020	.020	.020	.020	.020	.020

THE ABSOLUTE DIFFERENCE BETWEEN THE
CALCULATED AND EXPERIMENTAL INFILTRATION CURVES IS 1.5089

APPENDIX C

TEST DATA

Test No. 1
(Medium Sand)

Time (min)	Rate (cm/hr)	Vol. (cm)
0.0	5000.0	0.00
.1	325.0	.85
.5	200.0	2.40
1.0	145.0	3.75
2.0	113.0	5.90
3.0	98.0	7.60
4.0	89.0	9.20
5.0	83.0	10.60
6.0	77.4	12.00
7.0	73.2	13.20
8.0	70.0	14.30
9.0	67.0	15.50
10.0	65.0	16.60

Test No. 2
(Medium Sand)

Time (min)	Rate (cm/hr)	Vol. (cm)
0.0	5000.0	.0
.5	212.0	2.6
1.0	170.0	4.2
2.0	138.0	6.7
3.0	120.0	8.7
4.0	110.0	10.5
5.0	102.0	12.3
6.0	97.0	14.0
7.0	91.0	15.7
8.0	88.0	17.0
9.0	85.0	18.5
10.0	83.0	20.0

Test No. 3
(Medium Sand)

Time (min)	Rate (cm/hr)	Vol. (cm)
0.0	5000.0	0.0
1.0	90.0	3.4
2.0	60.0	4.6
3.0	50.0	5.6
4.0	42.0	6.3
5.0	36.0	6.9
6.0	33.0	7.5
7.0	30.0	8.0
8.0	29.0	8.5
9.0	27.0	9.0
10.0	25.0	9.4

Test No. 4
(Medium Sand)

Time (min)	Rate (cm/hr)	Vol. (cm)
0.0	2000.0	0.00
.5	138.0	1.48
1.0	119.3	2.53
2.0	102.0	4.40
3.0	93.0	6.00
4.0	88.0	7.50
5.0	83.5	8.90
6.0	80.0	10.10
7.0	77.0	11.50
8.0	75.0	12.70
9.0	74.0	14.00
10.0	72.0	15.00

Test No. 5
(Fine Sand)

Time (min)	Rate (cm/hr)	Vol. (cm)
0.0	2000.0	0.00
1.0	39.0	1.30
2.0	27.5	1.85
3.0	22.5	2.27
4.0	19.5	2.65
5.0	17.5	2.95
6.0	16.0	3.22
7.0	14.8	3.55
8.0	13.8	3.80
9.0	13.0	4.00
10.0	12.5	4.12
12.0	11.3	4.65
15.0	10.2	5.30
20.0	8.8	6.20